UNIVERSIDADE FEDERAL DO CEARÁ
CENTRO DE CIÊNCIAS
DEPARTAMENTO DE BIOQUÍMICA E BIOLOGIA MOLECULAR
PROGRAMA DE PÓS-GRADUAÇÃO EM BIOQUÍMICA

IGOR RAFAEL SOUSA COSTA

Análise dos perfis metabólicos de porta-enxertos de *Vitis* sp cocultivados com o fungo *Fusarium oxysporum* como estratégia para seleção de biomarcadores

FORTALEZA - CE
2022

IGOR RAFAEL SOUSA COSTA

ANÁLISE DOS PERFIS METABÓLICOS DE PORTA-ENXERTOS DE VITIS SP COCULTIVADOS COM O FUNGO *Fusarium oxysporum* COMO ESTRATÉGIA PARA SELEÇÃO DE BIOMARCADORES

Dissertação apresentada ao programa de pós-graduação do Departamento de Bioquímica e Biologia Molecular da Universidade Federal do Ceará como requisito para a obtenção do grau de mestre em bioquímica. Área de concentração: Bioquímica Vegetal.

Orientador: Prof. Dr. Humberto Henrique de Carvalho.

FORTALEZA - CE
2022

Dados Internacionais de Catalogação na Publicação
Universidade Federal do Ceará
Sistema de Bibliotecas
Gerada automaticamente pelo módulo Catalog, mediante os dados fornecidos pelo(a) autor(a)

C872a Costa, Igor Rafael Sousa.
Análise dos perfis metabólicos de porta-enxertos de Vitis sp cocultivados com o fungo Fusarium oxysporum como estratégia para seleção de biomarcadores / Igor Rafael Sousa Costa. – 2022.
73 f. : il. color.

Dissertação (mestrado) – Universidade Federal do Ceará, Centro de Ciências, Programa de Pós-Graduação em Bioquímica, Fortaleza, 2022.
Orientação: Prof. Dr. Humberto Henrique de Carvalho..
Coorientação: Prof. Dr. Kirley Marques Canuto .

1. Vine. 2. Rootstocks. 3. BDMG-573. 4. Paulsen-P1103. 5. Metabolome. I. Título.

CDD 572

IGOR RAFAEL SOUSA COSTA

ANÁLISE DOS PERFIS METABÓLICOS DE PORTA-ENXERTOS DE *Vitis sp* COCULTIVOS COM O FUNGO *Fusarium oxysporum* COMO ESTRATÉGIA PARA SELEÇÃO DE BIOMARCADORES

Dissertação apresntada ao programa de pós-graduação em Bioquímica do Departamento de Bioquímica e Biologia Molecular da Universidade Federal do Ceará como requisito para a obtenção do grau de mestre em bioquímica. Área de concentração: Bioquímica Vegetal.

Aprovado em: ___/___/_____.

BANCA EXAMINADORA

_____
Prof. Dr. Humberto Henrique de Carvalho (Orientador)
Universidade Federal do Ceará (UFC)

_____
Prof. Dr. Kirley Marques Canuto (Coorientador)
Embrapa Agroindústria Tropical (Fortaleza-CE)

_____
Prof. Dr. Murilo Siqueira Alves
Universidade Federal do Ceará (UFC)

_____
Dr. Paulo Riceli Vasconcelos Ribeiro
Embrapa Agroindústria Tropical (Fortaleza-CE)

AGRADECIMENTOS

Primeiramente a Jeová Deus, por me sustentar ao longo dessa caminhada iluminando os meus passos!

Aos meus pais, Evanildo Sousa e Estrela Costa, meus maiores exemplos da minha vida que, com muita dedicação, paciência e perspicácia, sempre me mostraram a importância de seguir os caminhos da honestidade, do trabalho árduo e do bom caráter, além do apoio necessário em muitos momentos. A vocês, minha eterna e profunda gratidão.

Ao amor da minha vida Geovana Sampaio, minha estimada esposa e amiga, que sempre me deu apoio em palavras e ações, por acreditar no meu potencial em realizar meus objetivos e que nunca me deixou desanimar nos momentos difíceis.

Aos meus amados irmãos Rômulo Costa e Jéssica Costa com seus respectivos cônjugês, pelas palavras de apoio e por confiar na minha capacidade de chegar até aqui.

Como as sábias palavras do Rei Salomão no livro de provérbios 17:17: "O verdadeiro amigo ama em todos os momentos e se torna um irmão em tempos de aflição", é com esse versículo que expresso minha gratidão aos amigos que conquistei no LabFive durante essa etapa e que compartilhei momentos de risadas, experiências, superações e desabafos: Lucas Pacheco, Dalton Oliveira, Stelamaris Paula, Karol Roger, Marta Noronha, Jessimiel, Sávio e Micaelly.

Aos meus amigos Fernando, Jefferson, Robherwal Filho, Oberdan, Gabrielle, Isabelle, pelo apoio e incentivo.

Aos colegas e pesquisadores da Embrapa que me acompanharam durante toda essa trajetória, trocando experiências e aprendizados: Sheyla, Kaline, Élder, Prof.Dr. Edir, Prof.Dr. Cleberson e especialmente ao Dr. Paulo Ricceli por todo o apoio técnico e científico para o desenvolvimento deste trabalho e por aceitar participar da banca examinadora contribuindo através dos seus conhecimentos com a melhoria do trabalho. Muito obrigado!

Ao Dr. Fabio Rossi, pela a idéia inovadora e desenvolvimento desse trabalho. Agradeço por todo o apoio e conselhos nessa trajetória.

Em especial, expresso minha profunda gratidão ao meu orientador Prof. Dr. Humberto Henrique de Carvalho pela orientação, paciência, disponibilidade, conselhos, e por sempre acreditar no potencial de todos os seus orientandos. Espero que possamos continuar essa parceria! Muito obrigado.

Meus mais sinceros agradecimentos ao meu coorientador professor Kirley Marques Canuto, pela paciência, orientação e por ser um exemplo de excelência na dedicação à pesquisa científica! Obrigado pelos ensinamentos.

Ao professor Prof. Dr. Murilo Siqueira Alves, por aceitar a participar da banca examinadora contribuindo singularmente na qualidade desse trabalho.

Ao Prof. Dr. Enéas Gomes-Filho e ao Prof.Dr. Lineker de Sousa Lopes por, contribuir com os seus conhecimentos para a melhoria do trabalho. Muito obrigado!

A Universidade Federal do Ceará, Centro de Ciências, Coordenação do PPGB e aos professores e técnicos do Departamento de Bioquímica e Biologia Molecular, pela excelência e qualidade no ensino, proporcionando condições para que este trabalho fosse realizado.

Aos meus colegas de trabalho da Escola Santa Luzia e ao Governo do Estado do Ceará/Sefor 2 por permitir o afastamento para melhor me dedicar aos estudos e assim capacitar seus professores para melhor servir na qualidade de ensino das escolas públicas.

A Coordenação de Aperfeiçoamento de Pessoal de Nível Superior (CAPES), pela concessão de bolsa de mestrado, a EMBRAPA Uvas e Vinhos por fornecer o material vegetal e a EMBRAPA Agroindústria Tropical pelo apoio técnico-financeiro (SEG 22.16.04.035.00.00) fundamental para o desenvolvimento dessa pesquisa.

A todos os doutorandos e mestrandos parceiros que, de alguma forma, contribuíram para a realização deste trabalho. Muito Obrigado!

RESUMO

A videira é uma das principais frutíferas do mundo e suscetível a muitas infecções, especialmente fungos como *Fusarium oxysporum*. A busca por genótipos e o uso de porta-enxertos mais tolerantes se tornou uma estratégia para minimizar este problema. Assim, o objetivo desse trabalho foi a partir de uma metabolômica global não direcionada, estudar os perfis metabolicos de porta-enxertos (Paulsen 1103 e BDMG573) co-cultivados com *F. oxysporum* e assim identificar marcadores bioquímicos de curto, médio e longo prazo de infecção (0, 4 e 8 dias após infecção - DAT). Na parte aérea, há sobreposição entre os tratamentos CNT e FUS do genótipo BDMG573 no 0 DAT e maior distinção em 4 DAT e 8 DAT (15 e 20 metabólitos significantes). No P1103 ocorreu uma maior diferença entre tratamentos no 0 DAT (21 metabólitos), seguido de maior sobreposição em 4 DAT e 8 DAT. Nas raízes, maiores similaridades entre os dois tratamentos de cada genótipo ocorreram no 0 DAT. Aos 4 DAT e 8 DAT, perfis distintos foram observados no BDMG573 (28 e 32 metabólitos) e P1103 (16 e 26 metabólitos). OPLS-DA identificou potenciais biomarcadores, na parte aéra do BDMG573 destacam-se a 1,3-dihidroxicetona (0 e 4 DAT) e a maltose (4 e 8 DAT) enquanto que no P1103 destacam-se ácidos orgânicos no 0 DAT (ácido glicérico), aminoácidos no 4 DAT (prolina) e carboidratos no 8 DAT (sorbitol). Nas raízes do BDMG573 destacam-se β-alanine (0 DAT), celobiose e sorbitol (4 e 8 DAT) e no P1103 os potenciais marcadores foram carboidratos como galactose (0 e 4 DAT) e 1,3-dihidroxicetona (8 DAT). Em geral, esse trabalho descreve a modulação de metabólitos primáios em genótipos tolerante e sensíveis de videiras ao fungo *F. oxysporum.* Assim, espera-se que esses dados poderão contribuir para estratégias de seleção assistida para aumento da tolerância em diferentes fases da infecção, bem como a identificação precoce da doença.

Palavras-chaves: Videiras; Porta-enxertos; BDMG-573, Paulsen-P1103, Metaboloma

ABSTRACT

The vine is a widespread fruit tree susceptible to many diseases caused by fungi such as *Fusarium oxysporum*. The search for tolerant rootstocks genotypes and has become a strategy to minimize this problem. Thus, the main goal of this work was to study the primary metabolism modulation of two rootstocks Pausen 1103 and BDMG573 co-cultured with *F. oxysporum*. Undirected global metabolomics identified biochemical markers of the early, medium, and late times (0, 4, and 8 days after infection - DAT). In the shoots, there was an overlapping between the CNT and FUS treatments of BDMG573 genotype at 0DAT and a better distinction at 4DAT and 8 DAT (15 and 20 significant metabolites). In P1103, there was a better distinction between treatments at 0 DAT (21 metabolites), followed by overlapping at 4 DAT and 8 DAT. In the roots, similarities between the two treatments of each genotype occurred at 0 DAT. Otherwise, there are distinct profiles between CNT and FUS of BDMG573 (28 and 32 metabolites) and P1103 (16 and 26 metabolites) at 4 DAT and 8 DAT, respectively. OPLS-DA multivariate analysis identified 1,3-dihydroxyacetone (at 0 and 4 DAT) and maltose (at 4 and 8 DAT) as potential biomarkers in the BDMG573 shoots. While in the shoots of P1103, some organic acids stand out at 0 DAT (glyceric acid), amino acids at 4 DAT (proline), and carbohydrates at 8 DAT (Sorbitol). In the roots of BDMG573, the metabolites β-alanine (at 0 DAT) and cellobiose and sorbitol (at both 4 and 8 DAT) stand out as potential biomarkers of Fusarium co-culture. While in the roots of P1103, the potential discriminants were carbohydrates such as galactose (at both 0 and 4 DAT) and 1,3-dihydroxyacetone (at 8 DAT). The pathways showed a increase of amino acids, glycolise, and components particularly in shoots of Pausen P1103 at all times evaluated. Overall, this work provides a new perspective of the primary metabolism modulation of tolerant and sensitive grapevine genotypes to the fungus F. oxysporum. Thus, it may contribute to assisted selection strategies for increasing genotypes tolerance and the early identification of the disease.

Keywords: Vine; Rootstocks; BDMG-573, Paulsen-P1103, Metabolome.

LISTA DE ABREVIATURAS E SIGLAS

ANOVA	Análise de variância unilateral
ANA	ácido naftalenoacético
BDA	batata dextrose ágar
BDMG-573	Bordô (*Vitis labrusca*) x Magnólia (*Vitis rotundifolia*
CNT	Controle (não co-cultivado)
Da	Daltons (massa molecular)
DAT	dias após o tratamento
DIC	delineamento inteiramente causalizado
EROs	espécies reativas de oxigênio
EM/MS	Espectômetro de massas
EMBRAPA	Empresa Brasileira de Pesquisa Agropecuária
eV	Elétron volt
Fo/FUS	*Fusarium oxysporum*
GABA	ácido gama-aminobitírico
GC	Cromatografia Gasosa
GMD	Golm Metabolome Database
HCA	Análise de cluster hierárquica
KEGG ID	Enciclopédia de Genes e Genomas de Kyoto
MSTFA	N-methyl-N-(trimethylsilyl)-trifluoro acetamide
MAMPs	*microbe - associated molecullar patterns*
MAPKs	fosforilação de proteínas quinases
OPLS-DA	Análise Discriminante de Mínimos Quadrados Parciais Ortogonais
PCA	Principal Component Analysis
PCR	Proteína C reativa
PLS-DA	Análise Discriminante de Mínimos Quadrados Parciais
PRRs	*pattern recognition receptor*
PTFE/L	Politetrafluoretileno hidrofílico
PTI	*pathogen- or pattern-triggered immunity*
P1103	'Paulsen'
TCA	ciclo do ácido tricarboxílico

SUMÁRIO

1 INTRODUÇÃO

1.1 Cultivo da videira

O gênero *Vitis* L. (videiras), com 80 espécies conhecidas, é o mais utilizado na viticultura (OIV, 2019) e cultivado há mais de 7.000 anos (MULLINS et al., 1992). Os pomares de *Vitis vinifera* L. (videira comum) são plantados em todo o mundo e têm um alto valor comercial para produção de uvas frescas de mesa, frutas secas e vinho. O cultivo de *V. vinifera* se concentra principalmente no Mediterrâneo e em outras regiões de clima temperado, entre as latitudes 30° e 50° nos hemisférios norte e sul (GRAMAJE; URBEZ-TORRES; SOSNOWSKI, 2018). Como resultado de seu fácil cultivo, longevidade dos vinhedos e inúmeras aplicações, em 2018, a área de superfície global para a produção de videira era de 7,4 milhões de hectares. (OIV, 2019 ; OIV, 2020). Outras espécies de *Vitis*, bem como seus híbridos interespecíficos, também são importantes para a produção de suco, uvas de mesa ou vinho e, em particular, para o desenvolvimento de porta-enxertos (GRAMAJE; URBEZ-TORRES; SOSNOWSKI, 2018).

As videiras (*V. vinifera* e *Vitis spp*.) são uma das culturas frutíferas lenhosas perenes mais extensamente cultivadas e economicamente importantes do mundo (GRAMAJE; URBEZ-TORRES; SOSNOWSKI, 2018). O continente europeu, com 3,55 milhões hectares e 28,9 milhões toneladas, lidera a produção mundial de uva e é seguida pela Ásia (2,04 milhões de ha), América do Sul (0,53 milhões de ha), América do Norte (0,43 milhões de ha), África (0,33 milhões de ha) e Oceania (0,18 milhões de ha) (FAO, 2017). Seis países respondem por aproximadamente 60% da produção mundial de uvas, incluindo a China (12,54 milhões de toneladas), EUA (7,12 milhões de t), Itália (6,93 milhões de t), Espanha (6,22 milhões de t), França (6,17 milhões t) e Turquia (4,17 milhões t) (FAO, 2017).

Figura 1 – Mapa dos maiores produtores mundial de vinho. Europa maior produtor, seguido da Ásia e Estados Unidos (EUA). Elaborada pelo prórpio autor.

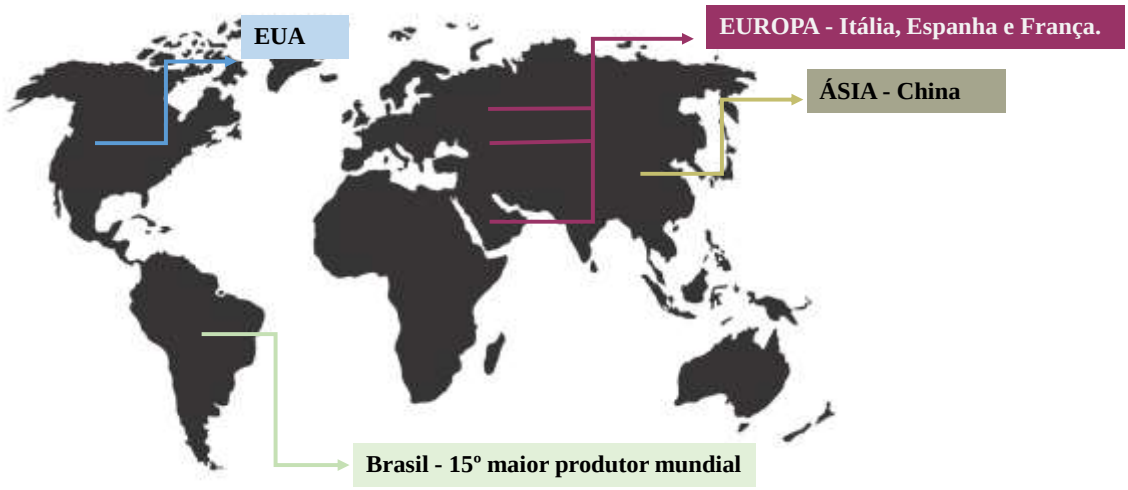

1.1.1 Importância vitivinicultura no Brasil

A vitivinicultura no Brasil se constitui em uma importante fonte de renda na maioria das regiões produtoras de uvas, principalmente onde predomina a agricultura familiar. Ela apresenta características regionais distintas, com particularidades no ciclo de produção, época de colheita, cultivares, tratos culturais, tipo de produto e foco demercado. Em algumas regiões convivem pequenas, médias e grandes propriedades vitícolas, cuja atividade têm contribuído com a sustentabilidade da vitivinicultura na geração de empregos e renda (MELLO; MACHADO, 2020).

A maior área cultivada com videiras está concentrada na região Sul, com 55.501 ha, representando cerca de 73% da área vitícola do país. Essa região é a maior produtora de uvas contribuindo para 53% da produção nacional. A maior parte da produção de uvas é do grupo americanas e híbridas, destinadas principalmente ao processamento para elaboração de vinhos de mesa e suco de uva (IBGE, 2020).). Além disso, a região Nordeste possui 10.485 ha de videiras, correspondendo aproximadamente 14% da área vitícola nacional (IBGE, 2020). Essa produção se concentra no Vale do São Francisco (Pernambuco e Bahia), que pelo fato de render até 2,5 safras por ano, na mesma área, sua importância nacional relativa gira em torno de 25%. Mas a produtividade do

vinho nacional vem sofrendo dificuldades que limitam sua competividade no mercado interno e externo. Segundo Cella et al 2021, o Brasil produziu 3,6 milhões de hectolitros de vinho classificando-o como 15º maior produtor mundial no ano de 2017 e exportando aproxidamente US$ 8 milhões no mesmo ano (OEC, 2019). Em 2018, o faturamento com exportações foi de aproximadamente de US$ 9 milhões, o que manteve baixa a participação no mercado externo, representado 0,02% das exportações mundiais. Mesmo assim, o mercado brasileiro de vitivinicultura emprega um boa atividade econômica e social relacionados a sustentabilidade de pequenos produtores, ampliando o número de postos de trabalho e gerando renda (HOECKEL; FREITAS; FEISTEL, 2017).

1.1.2 Fatores que afetam a produtividade dos vinhedos

Atualmente as mudanças climáticas são uma das principais preocupações globais que afetam a viticultura (BERNARDO et al., 2018). Condiçoes metereológicas ideais são condicionadas basicamente à irrigação ou ocorrência de chuvas que não comprometam o crescimento das plantas e qualidade enológica, além da ausência de temperaturas extremamente baixas (10.5 °C) e predominância de uma temperatura noturna mais amena (JUNGES; SANTOS; GARRIDO, 2022).

O uso de porta-enxertos adequados é uma estratégia de longo prazo para sobrevivencia às mudanças das condições climáticas, pois podem mitigar os estresses ambientais por se adaptarem às condições adversas do clima e do solo (CRAMER, 2010; FRAGA et al., 2016). A formação de um porta-enxerto de videiras geralmente é feita atraves do enraizamento de estacas, dependentes de fatores genéticos, nutricionais, hormonais, entre outros, sendo a maior capacidade de enraizemento de algumas espécies fundamental para o sucesso da técnica (WURZ; FELDBERG; BRIGHENTI, 2022). Um porta-enxerto ideal deve ter capacidade para tolerar seca, calor, salinidade, frio, insetos e pragas, bem como ser capaz de se adaptar a uma ampla gama de solos (OLLAT et al., 2016). Antes de selecionar e propagar um porta-enxerto de videira, alguns de seus atributos e características devem ser avaliados e levados em consideração, como compatibilidade, vigor, rendimento, capacidade de enraizamento, técnica de propagação e também adaptação ao solo e clima (PAVLOUSEK, 2011; PEDERSEN, 2006). Dentre aqueles mais tradicionais e amplamente recomendados está o ‘Paulsen 1103’ (*V. Berlandieri* x *V. rupestris*) caracterizado pela tolerância à fusariose, enquanto que outros estão ainda em fase de experimentação como o BDMG573/BM573 (*V. lambruscana*

‘Bordo’ x *V. rotundifolia* ‘Magnólia’) (Figura 2) devido à conhecida tolerância dos parentais e alta capacidade de enraizamento (CAVALCANTI, 2021; COSTA; LOVATO; SETE, 2010; GARRIDO; SÔNEGO; GOMES, 2004b; REINHART, 2013).

Figura 2 – (A) Genótipos de *Vitis* BDMG573 e P1103 em diferentes dias de infecção. (B) Porcentagem do grau de severidade da doença e comparação dos dois genótipos (CAVALCANTI, 2021)

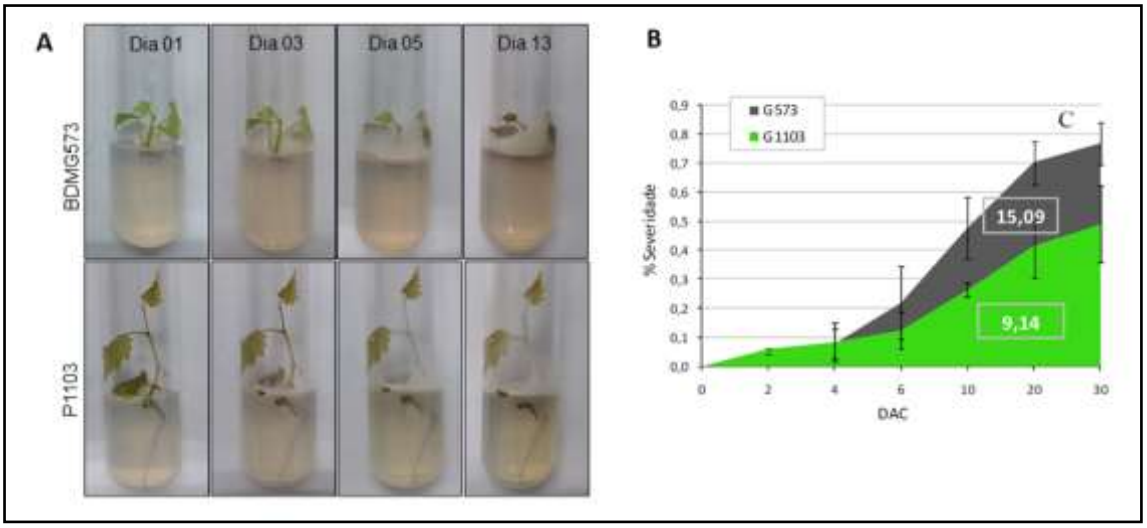

A videira está sujeita ao ataque de diversas doenças e pragas, as quais reduzem a quantidade e a qualidade da uva produzida, e em muitos casos podem inviabilizar a cultura. Essa suscetibilidade ao ataque de uma ampla gama de fitopatógenos que comprometem a produtividade e a longevidade das videiras, afetam a capacidade de enraizamento, a arquitetura e a vitalidade das plantas e, por fim, resultam em mortalidade(KHAN et al., 2020). A cultura da vinha demanda um elevado investimento financeiro inicial para a implantação do pomar e onerosas operações anuais necessárias à produção. Uma parte significativa desses custos está associada a programas intensos de manejo de pragas e doenças, que incluem práticas culturais e o custo de produtos químicos e/ou de controle biológico e sua aplicação (WUNDERLICH; KLONSKY; STEWART, 2015). Isso é particularmente importante para o controle de doenças, pois *V. vinifera* é conhecida por apresentar vários patógenos vasculares através de lesões mecânicas, como feridas de poda (MUNDY; MANNING, 2010; ROLSHAUSEN et al., 2010; ÚRBEZ-TORRES; GUBLER, 2011). Entre eles, os patógenos fúngicos são de importância significativa, uma vez que *V. vinifera* é suscetível a 29 doenças fúngicas (WILCOX et al., 2015), incluindo doenças do tronco da videira (*Grapevine Trunk Diseases* - GTDs), que atualmente são consideradas uma das mais destrutivas (BERTSCH et al., 2013). Em razão disso, uso de porta-enxertos tolerantes tem ajudado a minimizar esse problema.

O número de casos de declínio e morte de plantas de videira tem sido um problema há muitos anos, causando grande redução de produtividade e de qualidade da uva. Segundo Garrido (2004), os principais agentes causais identificados associados a este problema são: pérola-da-terra (*Eurhizococcus brasiliensis* Hempel), fusariose (*Fusarium oxysporum* Schl. f.sp. *herbemontis* Tocchetto), fungos que causam podridão radicular [*Verticillium* sp., *Rosellinia necatrix Prill*., *Armillaria mellea* (Vahl:Fr.) P. Kumm e *Phytophthora* sp.], e os fungos que causam apodrecimento de tronco e ramos [*Botryosphaeria* sp., *Eutypa lata* (Pers.: fr.) Tul. & C. Tul., *Phomopsis viticola* (Sacc.) Sacc. E *Stereum* sp.] (GARRIDO; SÔNEGO, 1999; GARRIDO; SÔNEGO; GOMES, 2004a)

1.1.3 Interações planta-patógeno

Os pesquisadores há muito tentam entender os mecanismos pelo qual os fungos *Fusarium* causam sintomas como murcha nas plantas e apresentam especificidade de hospedeiro como formas (*formae speciales*) e raças (ARIE, 2019). Na década de 80, muitas abordagens bioquímicas e citológicas sugeriram vários fatores relacionados à patogenicidade. Por exemplo, Beckman (1989) descreveu a infecção por *F. oxysporum* (Fo) pela presença de enzima poligalacturonase (PGase). Já na década de 90, técnicas moleculares como amplificação de fragmentos de DNA por PCR, e análises de expressãogênica ajudaram a identificar o *pg1* como o primeiro gene determinante relacionado à patogenicidade em *F. oxysporum* (ARIE et al., 1998). A detecção das doenças nas videiras quando infectadas por um patógeno não é fácil de perceber principalmente nas primeiras horas após o contato. Pois antes que os sintomas da doença possam ser observados, ocorre uma complexa interação entre o agente causal e a videira que antecede a expressão dos sintomas (DE LAMO; TAKKEN, 2020; MUNDY; MANNING, 2010). A infecção é caraterizada como bem-sucedida por um patógeno quando ocorre a superação das defesas do hospedeiro. Mesmo quando os patógenos infectam com sucesso o sistema vascular das videiras, a expressão dos sintomas não é frequentemente observada na primeira estação, podendo não ter reduzido de tamanho nem apresentar sintomas na temporada seguinte (MUNDY; MANNING, 2010).

As raízes das plantas reconhecem os microrganismos por meio de padrões moleculares associados a micróbios (*microbe - associated molecullar patterns* - MAMPs) que estão presentes em patógenos e não patógenos (HACQUARD et al., 2017; HENRY;

THONART; ONGENA, 2012). O resposta de MAMPs é mediado por uma grande família de receptores de reconhecimento de padrões (*pattern recognition receptor* - PRRs), como por exemplo receptores de peptideoglicanos e quitina fúngicos, que ativam uma ou mais vias de sinalização (MACHO; ZIPFEL, 2014). PRRs são expressos principalmente em raízes com zonas vulneráveis à entrada de patógenos, resultando em uma heterogeneidade e responsividade específica do tecido a diferentes MAMPs (CHUBERRE et al., 2018). As várias respostas à quitina são principalmente circunscritas à zona madura, contudo as outras partes da raiz são relativamente insensíveis a estes MAMPs e não apresentam respostas imunes após a exposição à quitina (COLEMAN et al., 2019). Nas zonas responsivas, o reconhecimento MAMP (Figura 3) resulta na ativação de imunidade acionada por padrão (*pathogen- or pattern-triggered immunity* - PTI), que confere resistência a uma ampla variedade de patógenos potenciais (BIGEARD; COLCOMBET; HIRT, 2015). A ativação de PTI induz uma variedade de respostas de sinalização precoces, como um influxo de Ca^{2+} e H^{+} celular resultando em alcalinização do apoplasto, produção de espécies reativas de oxigênio (EROs) e fosforilação de proteínas quinases associadas a mitógenos (MAPKs) (BIGEARD; COLCOMBET; HIRT, 2015; CHUBERRE et al., 2018). As EROs, além de moléculas de sinalização, têm efeitos tóxicos diretos sobre os micróbios (O'BRIEN et al., 2012) e podem induzir a morte celular, limitando assim a progressão de patógenos (DE LAMO; TAKKEN, 2020; MUR et al., 2008). Além de PTI, fitohormônios como ácido salicílico (SA), ácido jasmônico (JA) e etileno (ET), também estão envolvidos na defesa da raíz contra patógenos (CHEN et al., 2019; PAPADOPOULOU et al., 2018).

Figura 3 – Padrões moleculares associados a patógenos (PAMP) desencadeada por imunidade por patógeno ou padrão (PTI) e imunidade por efetores (ETI) para diferentes tipos de (MAMPs) padrões moleculares moleculares associados a micróbios, (DAMPs) padrões moleculares associados a danos e (HAMPs) padrões moleculares associados a herbívoros (MALIK; KUMAR; NADARAJAH, 2020).

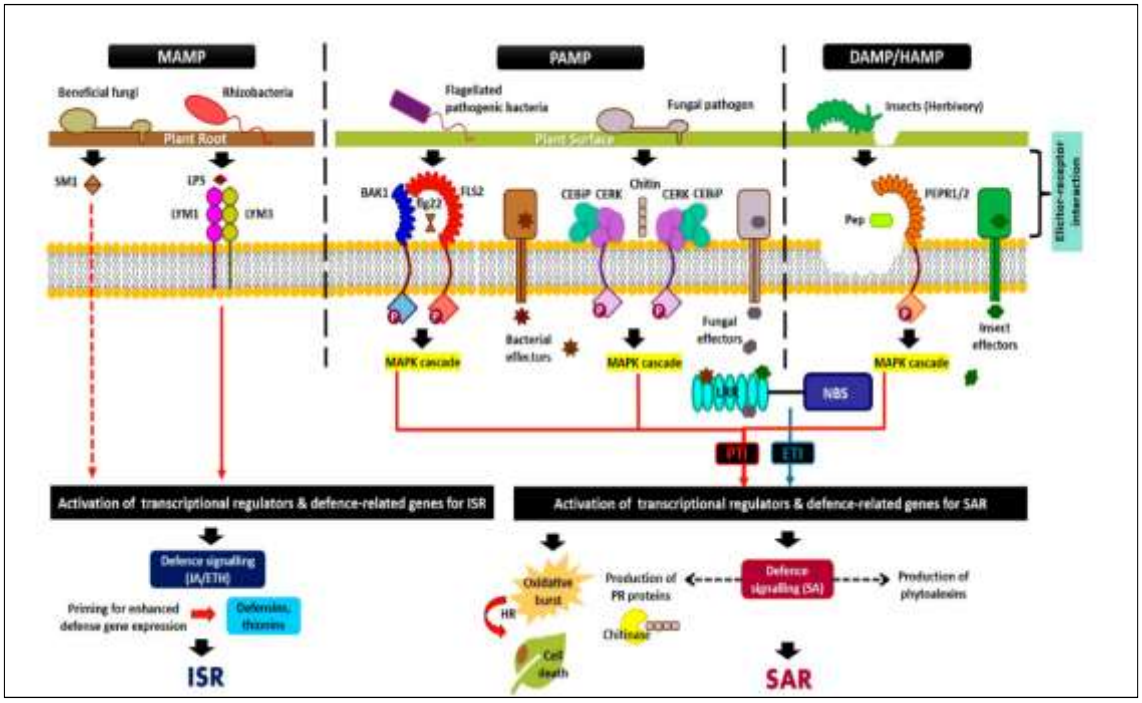

1.2 Gênero *Fusarium*

O gênero *Fusarium* consiste em um grande número de patógenos oportunistas que infectam várias espécies de plantas em uma variedade de zonas climáticas (por exemplo, complexo de espécies *F. graminearum*, complexo de espécies *F. fujikuroi*, complexo de espécies *F. equiseti*, *F. avenaceum* e *F. culmorum*), e alguns são mais típicos do solo, e são provavelmente mais isolados da rizosfera de plantas, principalmente complexo de espécies *F. oxysporum* e complexo de espécies *F. solani* (WAALWIJK et al., 2004). Alguns complexos de *Fusarium* ainda são classificados como grupos especializados dentro da espécie, chamadas *formae specialis* (f.sp.) com base no hospedeiro que são capazes de infectar. *F. oxysporum* (Fo) é a espécie com maior número de *formae specialis*. Por exemplo, *F. oxysporum* f.sp. *lycopersici* causa murcha no tomate, enquanto *F. oxysporum* f.sp. *cubense* causa a doença do Panamá na banana e *F. oxysporum* f.sp. *herbemontis* que causa lesões nos sistemas vascular e radicular de videiras, dentre outras (SUSCA; MORETTI; LOGRIECO, 2017). As espécies

pertencentes ao gênero *Fusarium* são geralmente saprotróficas, enquanto os necrotróficos são potencialmente patogênicos ou não são patogênicos obrigatórios. Algumas das espécies podem formar corpos de frutificação, que permanecem viáveis por um longo tempo e então germinam no aparecimento de condições adequadas para infectar as raízes das plantas (DWEBA et al., 2017; RONCERO et al., 2003). A elevada agressividade de infecção está relacionada a vários metabólitos secundários já caracterizados como micotoxinas: desoxinivalenol, zearalenona, toxina T-2 e fumonisina B1(Figura 4), que podem causar doenças em plantas, humanos e animais (ZHANG et al., 2020). Além disso, o ácido fusárico (ácido 5-butilpicolínico, FA) é uma das mais importantes micotoxinas não específicas de hospedeiro, produzida por todas as espécies de *Fusarium* e que desempenha um papel direto na atividade da patogênese por perturbar o metabolismo da planta infectada, levando à inibição de enzimas defensivas e redução da viabilidade celular das plantas hospedeiras (BOUIZGARNE et al., 2006; DING et al., 2018; ZHANG et al., 2020).

Figura 4 - Estrutura química das principais micotoxinas descritas no gênero *Fusarium* (ZHANG et al., 2020).

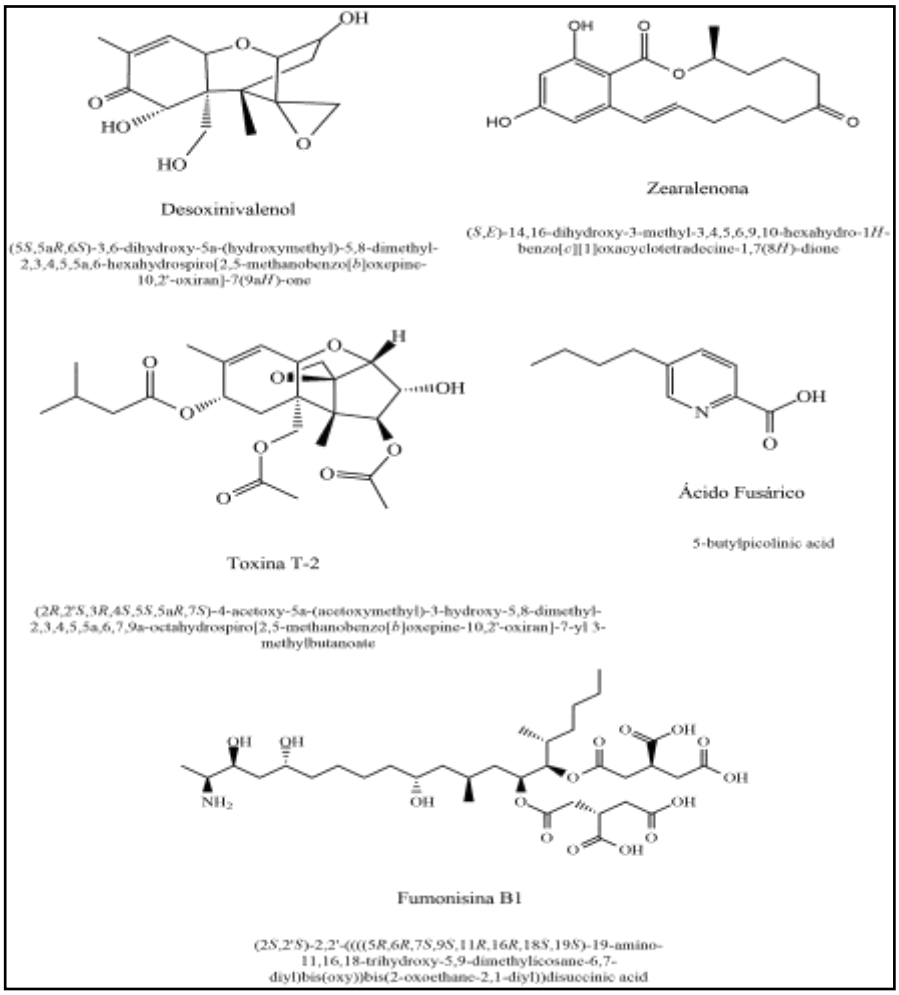

A germinação de esporos Fo ou hifas é a primeira fase do processo de colonização de uma raiz. Após a germinação, as hifas fúngicas colonizam as superfícies das raízes de plantas hospedeiras penetrando via feridas, rachaduras na epiderme, emergência lateral da raiz ou por penetração direta na ponta da raiz, colonizando o córtex (DE LAMO; TAKKEN, 2020; GORDON, 2017; HUMBERT et al., 2015). A quantidade de biomassa das cepas patogênicas nas raízes passa a aumentar, alcançando os vasos do xilema de onde elas colonizam os tecidos e seus estágios iniciais de crescimento se tornam aparentes (LANUBILE et al., 2015). As oclusões induzidas dos vasos do xilema visando restringir o progresso do patógeno resulta no murchamento, um sintoma conhecido de plantas infectadas (GORDON, 2017). Nas videiras, a espécie *F. oxysporum* Schl. f.sp. *herbemontis* penetra principalmente nos tecidos da raiz, o que pode levar à morte da planta (BRUM et al., 2012). Os sintomas podem ser lesões necróticas internas (Figura 5), bem como listras marrons no xilema externo (MONDELLO et al., 2018; MUGNAI; GRANITI; SURICO, 1999). A gravidade da doença aumenta quando as plantas são atacadas por insetos que produzem feridas, facilitando a infecção fúngica (BRUM et al., 2012; EDWARDS et al., 2007). A doença causada pelo fungo *F. oxysporum* Schl. f.sp. *herbemontis*, é nativa da região Sul do Brasil, ocorrendo no Rio Grande do Sul e em Santa Catarina. Também é importante salientar que a ocorrência desse patógeno, não impede o aparecimento de outras espécies de fungos nas videiras, tendo em vista a coleta de campo (GARRIDO; SÔNEGO; GOMES, 2004a).

Figura 5 - Necrose de tecidos lenhosos nas videiras afetadas (REVEGLIA et al., 2017).

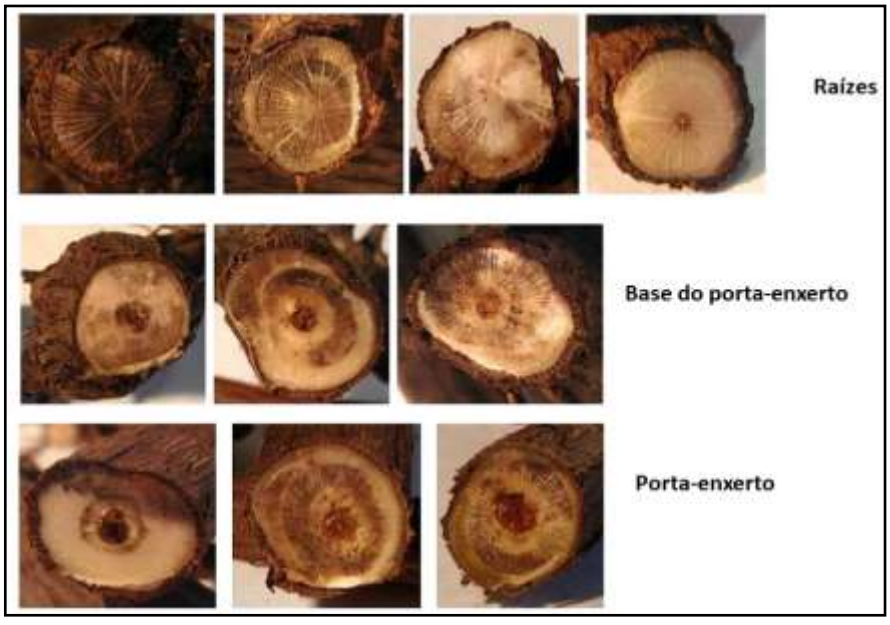

1.3 Metabolômica como estratégia para identificação de biomarcadores

Como estratégia de estudo, as ômicas têm contribuido para compreensão do funcionamento celular dos organismos e suas modificações biológicas, a nível molecular (FIEHN, 2002), dentre as quais, a metabolômica é o estudo das modulações em perfis metabólicos. O metaboloma representa o agrupamento de metabólitos de baixa massa molecular (até 1500 Da) e produtos intermediários ou finais do metabolismo em uma amostra biológica. Além disso, a literatura descreve outros conceitos no tocante ao campo dessa ciência, como por exemplo: o perfil metabólico consiste em uma análise de metabólitos previamente selecionados por vias bioquímicas específicas; o *fingerprinting* é caracterizada como uma classificação de amostras de acordo com sua origem ou sua magnitude biológica e a análise *footprinting* que se reporta aos metabólitos excretados por uma célula monitorada (KELL et al., 2005). De um modo geral, podemos classificar as análises metabolômicas em: metabolômica alvo**,** que é determinada por uma análise quantitativa de um ou mais metabólitos pré-selecionados de uma classe química estabelecida, ou que estejam ligados a vias metabólicas específicas, e a metabolômica global, que consiste na análise qualitativa da maior quantidade de metabólitos viáveis, referente a diversas classes químicas, incorporado ao sistema biológico em análise (KUEHNBAUM; BRITZ-MCKIBBIN, 2013).

Estudos entre as interações de planta-patógenos tem crescido na última década devido o impacto dos fungos fitopatogênicos na produtividade agrícola. Técnicas de metabolômica tem sido aplamente usadas em diferentes campos de pesquisa, como identificação de biomarcadores químicos, mecanismos de infecção e detecção de interações com o hospedeiro (BAIDOO, 2019; HEUBERGER et al., 2014). As análises metabolômicas das interações entre o patógeno e a planta têm sido realizadas principalmente entre vários fungos e suas plantas hospedeiras, especialmente entre *Fusarium graminearum*, *Magnaporthe oryzae*, *Ustilago maydis*, *Rhizoctonia solani*, *Botrytis cinerea*, e seus hospedeiros (CHEN; MA; CHEN, 2019). A literatura relata amplamente que o fungo *Fusarium* é um patógeno necrotrófico que secreta toxinas induzindo a morte dos tecidos das plantas e em seguida usa o tecido morto para obter os nutrientes durante a infeccção. Isso tem afetado não só o rendimento das colheitas mas também a qualidade dos produtos agrícolas (BAI; SHANER, 2004; CHEN; MA; CHEN, 2019). Se tratando do *Fusarium oxysporum*, a interação entre fungo e hospedeiro induz

mudanças no metabolismo primário, representado por uma ampla variação principalemente por açúcares, aminoácidos e ácidos orgânicos. De um modo geral, o patógeno ativa a transcrição de genes relacionados a alta demanda energética resultando em altos níveis de beta-amilase, sacarose sintase e invertase, para promover a maior disponibilidade de monssacarídeos como glicose e frutose. Em plantas mais tolerantes, a presença do patógeno é rapidamente detectada, o estabelecimento da infecção e a intensidade da resposta hipersensitiva são reduzidas e compensadas por sinais metabólicos primários no hospedeiro reduzindo o dano que seria gerado (GUPTA et al., 2010). Essas mudanças metabólicas têm relação com as variações de fluxos de carbono, enxofre e nitrogênio; o ciclo do ácido tricarboxílico (TCA); desvio do ácido gama-aminobitírico (GABA); via do chiquimato e aminoácidos, lipídios, colina, purinas, pirimidinas e outros metabólitos (BUHTZ et al., 2015; KUMAR et al., 2015).

Esses resultados sugerem que a metabolômica pode ser usada para obter o perfil do metabolismo primário, produzidos pelas plantas após a infecção de fungos patogênicos, sendo uma ferramenta eficaz para estudar as vias metabólicas, imunidade da planta e também para identificar fungos fitopatogênicos através dos seus metabólitos secundários (CHEN et al., 2019; FEUSSNER; POLLE, 2015; NAKABAYASHI; SAITO, 2015).

Os metabólitos secundários, são os mensageiros universais sendo o sinal de econhecimento do patógeno pela planta hospedeira e para ações do patógeno durante a infecção do hospedeiro. Eles pertencem a várias classes relativas às suas estruturas químicas e influenciam diversos processos bioquímicos, exibindo efeitos de sinalização, toxicidade, elicitação, *priming*, e ações promotoras de crescimento ou indutoras de resposta de defesa (DESJARDINS., 2006). A habilidade de produzir esses metabólitos é regulada pela presença e atividade de genes específicos nos genomas de fungos, que geralmente contêm vários códigos de enzimas dedicadas exclusivamente a biossintetizar grupos específicos de compostos (KOCZYK; DAWIDZIUK; POPIEL, 2015; PROCTOR et al., 2003, 2013; STĘPIEŃ, 2014). Muitos metabólitos secundários são universais para diversos microorganismos fúngicos, e suas ações são semelhantes para vários sistemas fitopatógenos; no entanto, um nível significativo de especificidade pode ser observado em análises comparativas metabolômicas de fungos patogênicos (ZHANG et al., 2020).

1.4 Análise pelo método CG-EM

A técnica analítica cromatografia gasosa acoplada à espectrometria de massas (CG-EM) consiste em um processo de separação entre uma fase estacionária (sólida ou líquida) e uma fase móvel, a qual é um gás de arraste (gás inerte) com a função de eluir os constituintes da mistura ao longo da coluna separando-os de acordo com suas afinidades. Amostras voláteis ou volatizadas (processo de derivatização) são injetadas na coluna e arrastadas em direção ao espectômetro de massas, onde serão ionizadas, analisadas e separadas de acordo com sua razão massa-carga (*m/z*) e transferidas ao detector que amplificará e transmitirá um sinal para o sistema de dados na forma de espectros de massas com seus valores de *m/z* e tempos de retenção (NASCIMENTO et al., 2018) .

A GC-EM é uma das técnicas de análise mais empregadas em estudos metabolômicos e apresenta alta robustez e reprodutibilidade. Análises de perfis metabólicos em CG-EM são comumente usadas em importantes grupos de metabólitos primários (ALSEEKH et al., 2021; CANUTO et al., 2018; FIEHN, 2008). Aminoácidos, açúcares e ácidos orgânicos formam uma importante classe de metabólitos, fundamentais para inúmeros processos bioquímicos (KHAKIMOV; JESPERSEN; ENGELSEN, 2014; KRUMPOCHOVA et al., 2015). Entretanto, grande parte dos metabólitos que compõem o metaboloma requerem derivatização, para que se tornem voláteis a baixas temperaturas (KOEK et al., 2011). O uso de GC-EM em metabolômica apresenta grandes vantagens tais como: alta resolução e sensiblidade. Tais características conferem credibilidade na identificação dos metabólitos, que combina a informação de tempo de retenção e o padrão de fragmentação obtido através de ionização por elétrons. Além de menor custo de operação em relação a outras formas de análises (BEALE et al., 2018).

A forma mais comum de detector usado em metabolômica baseada em CG-EM é a ionização eletrônica (EI). É considerado um método que leva à fragmentação reprodutível de moléculas em impressões digitais espectrais de massa bem caracterizadas por ser usada realizada a 70 eV (padrão) em instrumentos com diferentes analisadores de massa (YI et al., 2016). Esta padronização de ionização EI permite o uso de bibliotecas de espectro de massa, como o banco de dados de metaboloma GOLM publicamente disponível (GMD) e Instituto Nacional de Padrões e Tecnologia (NIST) Dados de Espectometria de Massas (BEALE et al., 2018; DANIEL et al., 2010).

1.5 Quimiometria : Análises Estatísticas Multivariadas

O uso de ferramentas quimiométricas são de grande importância, pois incluem métodos eficientes e robustos para modelagem, análise e interpretação de complexos químicos e dados biológicos. A quimiometria pode ser usada tanto para análise qualitativa como quantitativa dos dados experimentais (GRANATO et al., 2018). Métodos de análises estatística são apropriadamente usados tornando possível a visualização de dados complexos obtidos de estudos metabolômicos. Esses métodos podem ser supervisionados e não supervisionados (PILON et al., 2020; WIKLUND et al., 2008). As análises não supervisionadas (análise exploratória) visam o entendimento global da natureza do dado detectando tendências, agrupamentos ou padrões. Nas análises, os métodos não supervisionados disponíveis mais usados na metabolômica são: a análise de componente principal (PCA) e análise de cluster hierárquica (HCA). A análise PCA tem como princípio transformar as variáveis de alta dimensão contendo a maior variação, em pequenos números de fatores ortogonais denominados de PC's (GRANATO et al., 2018; OLIVERI; SIMONETTI, 2016). A PCA converte o conjunto de dados originais em duas matrizes distintas, conhecidas como matriz de *scores* e matriz de *loadings*. O gráfico de *scores* representa como as amostras interagem entre si em um espaço n-dimensional. Já o *loading* descreve como as variáveis dos dados originais estão combinadas nas PCs, indicando quais possuem maior contribuição para a formação de determinada PC. O HCA tem como objetivo agrupar amostras relativamente semelhantes em um cluster e relativamente diferentes em outro. Normalmente é disposto em dendogramas e pode apresentar desvantagem por não revelar a razão química dos agrupamentos, consequentemente dos metabólitos responsáveis pelo agrupamento de determinada amostra. Para tanto, é necessária a realização da HCA bidimensional (*clustergram*), em que é possível observar as principais variáveis responsáveis pelo agrupamento, como intensidade de um sinal em determinado deslocamento químico ou tempo de retenção (PILON et al., 2020; YI et al., 2016).

Por outro lado, as análises supervisionadas (análise discriminatória) têm como objetivo principal obter uma correlação de variáveis químicas e um conjunto de dados para a determinação de biomarcadores e metabólitos ativos. Dentre os mais usados que podem ser classificados como métodos lineares, como Análise Discriminante de Mínimos Quadrados Parciais (PLS-DA), e Análise Discriminante de Mínimos Quadrados Parciais Ortogonais (OPLS-DA) pois ambos forçam a separação dos dados em grupos

experimentais (PILON et al., 2020). Para melhor visualização e interpretação dos dados o OPLS-DA, a mais recente modificação de PLS-DA, tem sido amplamente aplicado na modelagem e descoberta de biomarcadores em metabolômica (YI et al., 2016). Afim de selecionar metabólitos estatisticamente relevantes, essas análises multivariadas consideram a Importância da Variável em Projeção (VIP), VIP > 1.0 (MEVIK; WEHRENS, 2007; THÉVENOT et al., 2015). A modelagem de dados metabolômicos é um tipo de trabalho sistemático. Para estudos exploratórios, métodos não supervisionados, como PCA, fornecem uma primeira olhada informativa nas estruturas e relacionamentos do conjunto de dados entre grupos. Em seguida, métodos supervisionados, como PLS-DA e OPLS-DA, são aplicados para classificar as amostras também como descobrir biomarcadores.

Diante disso, a pesquisa em estudo utilizou uma abordagem metabolômica global, com o intuito de obter marcadores químicos do metabolismo primário, que possam ajudar a compreender o mecanismo de resposta da dinâmica molecular de dois porta-enxertos de videiras (BDMG573 e Pausen 1103) co-cultivados com fungo *Fusarium oxysporum* f.sp. *herbemontis*. Espera-se que os resultados além de aprofundar os conhecimentos, possam ser utilizados como ferramentas na elaboração de estratégias de diagnósticos para controlar a doença na planta.

2 HIPÓTESE

A longo prazo, a melhor estratégia de manejo de *Vitis* sp é selecionar e desenvolver cultivares tolerantes à fusariose. Portanto, é importante entender os mecanismos bioquímicos envolvidos com a resposta à fusariose em vinhas. Diante do exposto levantou-se a hipótese que os genótipos Paulsen P1103 e BDMG753 com tolerância diferencial ao fungo *Fusarium oxysporum* f.sp. *herbemontis* apresentam diferentes perfis metabólicos em raízes e/ou nas folhas modulando marcadores bioquímicos/químicos em diferentes tempos de interação.

3 OBJETIVOS

3.1 Objetivo Geral

Estudar a modulaçao do metabolismo primário resultante da interação entre o fungo fitopatogênico *Fusarium oxysporum* Schl. f.sp. *herbemontis* e porta-exertos de videiras de genótipos com diferentes graus de suceptibilidade e em diferentes tempos de infecção através de metabolômica global, visando à identificação de potenciais moléculas químicas marcadoras.

3.2 Objetivos Específicos

- Determinar os perfis metabólicos das partes aéreas e raízes de dois genótipos de videiras em diferentes tempos de cultivo;
- Avaliar diferenças nos perfis desses tecidos com e sem o processo de co-cultivo com o fungo *Fusarium oxysporum*.
- Identificar marcadores químicos na parte aérea e raízes dos dois genótipos de videiras considerados tolerantes e sensíveis ao *F. oxysporum*;
- Identificar possíveis rotas metabólicas envolvidas no processo de cocultivo com o fungo.

4 MANUSCRITO

O manuscrito a seguir foi escrito em Inglês e será submetido em revista internacional *qualis* A1 de acordo com a CAPES.

Title: GC-MS based Metabolomic approach exhibits different profiles and potential biomarkers of *Vitis* genotypes co-cultivated with *Fusarium oxysporum* at early, medium and late times

Title page

GC-MS based Metabolomic approach exhibits different profiles and potential biomarkers of *Vitis* genotypes co-cultivated with *Fusarium oxysporum* at early, medium and late times

Igor Rafael Sousa Costa[1], Fabio Cavalcanti Rossi [2], Francisco Lucas Pacheco Cavalcanti[1], Enéas Gomes Filho[1], Kirley Marques Canuto[3], Humberto Henrique de Carvalho[1]

Affiliations

[1] Department of Biochemistry and Molecular Biology, Sciences Center, Federal University of Ceará – Campus do Pici, CEP: 60440-554, Fortaleza, Ceará - CE, Brazil,

[2] Embrapa Uva e Vinho, Rua Livramento, nº 515 Caixa Postal: 130 CEP: 95701-008 - Bento Gonçalves – RS, Brazil,

[3] Embrapa Agroindústria Tropical, Rua Dra. Sara Mesquita, 2270, CEP: 60511-110, Fortaleza, CE, Brazil

Abstract

The vine is a widespread fruit tree susceptible to many diseases caused by fungi such as *Fusarium oxysporum*. The search for tolerant rootstocks genotypes and has become a strategy to minimize this problem. Thus, the main goal of this work was to study the primary metabolism modulation of two rootstocks Pausen 1103 and BDMG573 co-cultured with *F. oxysporum*. Undirected global metabolomics identified biochemical markers of the early, medium, and late times (0, 4, and 8 days after infection - DAT). In the shoots, there was an overlapping between the CNT and FUS treatments of BDMG573 genotype at 0DAT and a better distinction at 4DAT and 8 DAT (15 and 20 significant metabolites). In P1103, there was a better distinction between treatments at 0 DAT (21 metabolites), followed by overlapping at 4 DAT and 8 DAT. In the roots, similarities between the two treatments of each genotype occurred at 0 DAT. Otherwise, there are distinct profiles between CNT and FUS of BDMG573 (28 and 32 metabolites) and P1103 (16 and 26 metabolites) at 4 DAT and 8 DAT, respectively. OPLS-DA multivariate analysis identified 1,3-dihydroxyacetone (at 0 and 4 DAT) and maltose (at 4 and 8 DAT) as potential biomarkers in the BDMG573 shoots. While in the shoots of P1103, some organic acids stand out at 0 DAT (glyceric acid), amino acids at 4 DAT (proline), and carbohydrates at 8 DAT (Sorbitol). In the roots of BDMG573, the metabolites β-alanine (at 0 DAT) and cellobiose and sorbitol (at both 4 and 8 DAT) stand out as potential biomarkers of Fusarium co-culture. While in the roots of P1103, the potential discriminants were carbohydrates such as galactose (at both 0 and 4 DAT) and 1,3-dihydroxyacetone (at 8 DAT). The pathway showed a increase of amino acids, glycolise, and components particularly in shoots of Pausen P1103 at all times evaluated. Overall, this work provides a new perspective of the primary metabolism modulation of tolerant and sensitive grapevine genotypes to the fungus F. oxysporum. Thus, it may contribute to assisted selection strategies for increasing genotypes tolerance and the early identification of the disease.

Keywords: Vine; Rootstocks; BDMG-573, Paulsen-P1103, Metabolome.

Introduction

The vine (*Vitis sp*) is a widespread fruit tree of cultural and economic importance since grapes, leaves, and seeds are the basis for food, beverages, medicinal products, and others (VENKITASAMY et al., 2019). Likewise to other plants, vines are susceptible to many trunk diseases, such as viruses, bacteria, and fungi, requiring intensive use of chemicals to limit the growth of pathogens (MONDELLO et al., 2018). These products result in high costs, and negative economic and environmental impacts, which lead to the search for alternative management strategies and obtaining hybrids plants by mixing different vine genotypes (VOLYNKIN et al., 2021). Thus, to control effectively the invasion of microbial pathogens, plants use pre-existing physical resources and chemical barriers as well as inducible defense mechanisms that comprise a hypersensitive response (HR), and systemic acquired resistance (SAR) activated upon attack (DURRANT; DONG, 2004).

Among the main microorganisms that provoke injury to plants, the soil fungus *Fusarium* is widely spread. It promotes wilt, decline, and death in several important crops, such as banana (ZHANG et al., 2019), melon (SEBASTIANI et al., 2017), tomato (LAGOPODI et al., 2002), Arabidopsis (KIDD et al., 2011), and grapevines (BRUM et al., 2012; REVEGLIA et al., 2017). As it is a necrotrophic pathogen, the responses of the defense mechanisms for each plant species to the respective types of *F. oxysporum* were hypersensitivity reactions, responses to root tissue injuries, enzymatic responses, gene expressions, and metabolic alterations (CHEN et al., 2019; VAN LOON; REP; PIETERSE, 2006). Particularly, the *F. oxysporum* Schl. f.sp. *herbemontis* (Fo) is originaly from South Brasil, it mainly penetrates in the grapevines root tissues, colonizes the xylem system blocking water transport to leaves which can lead to the plant death (ANDRADE et al., 1995; GARRIDO; SÔNEGO; GOMES, 2004b; ZIEDAN; EMBABY; FARRAG, 2011).

The use of suitable rootstocks is a long-term strategy to deal with biotic and abiotic stresses as they can tolerate adverse conditions (FRAGA et al., 2016; CRAMER, 2010). Among those genotypes there is the traditional and widely recommended ‘Paulsen 1103’ (*V. Berlandieri* x *V. rupestris*) characterized by its tolerance to fusariosis, while others are still experimental, such as BDMG573/BM573 (*V. lambruscana* ‘Bordo’ x *V. rotundifolia* ‘Magnólia’) due to known parental tolerance and

rooting potential (CAVALCANTI, 2021; COSTA; LOVATO; SETE, 2010; GARRIDO; SÔNEGO; GOMES, 2004b; REINHART, 2013).

The study on the biochemical and molecular adjustments of the plant response to biotic stresses may provide useful insights to decode the mechanisms involved in a plant-microbe interaction (WONG et al., 2019; XU et al., 2015). Furthermore, the metabolite responses can be used as biomarkers to indicate health or disease status in plants and give more information about the pathogenicity of the disease agent (SANKARAN et al., 2010; WONG et al., 2020). In this regard, metabolomics can be applied to detect developmental changes in the plant metabolome, metabolite functions, and metabolic pathways caused by the stimulation of pathogenic fungi favoring the development of new strategies to control fungal diseases (FEUSSNER; POLLE, 2015; NAKABAYASHI; SAITO, 2015; TAN et al., 2009). In addition, the presence of the pathogen is quickly detected by tolerant plants, and metabolic signals are triggered to contain the infection. It results in changes in the primary metabolism represented by a variety of sugars, amino acids, and organic acids. In general, there are changes in the source-drain relations due to high energy demand, which promotes the availability of monosaccharides such as glucose and fructose (GUPTA et al., 2010).

Metabolomics based on gas chromatography-mass spectrometry (GC-MS) is a qualitative large-scale analytical technique used to study several metabolites simultaneously in a complex mix of biological extracts. It has high robustness, reproducibility, sensitivity, and lower cost (ALSEEKH et al., 2021; BEALE et al., 2018). In the last decade, metabolomics techniques have been applied in the study of plant-pathogen fungal interactions aiming to clarify the mechanisms triggered in the host that help the plant defense (CHEN; MA; CHEN, 2019). Indeed, GC-MS identified the increase of primary metabolites upon *F. oxysporum* infection, in which amino acids and sugars act as energy or signaling molecules with a role in innate defense pathways (CHEN et al., 2019; GUPTA et al., 2010). Further, metabolic profiles of plants with fusariosis vary according to genotypes and tissues. Metabolites such as arginine, aspartic acid, histidine, valine, and lysine were described for monitoring the disease in watermelon plants (KASOTE et al., 2020).

Therefore, the main goal of this work was to study the primary metabolism in the plant-pathogen interaction of two vine genotypes with a previously described differential susceptibility to the phytopathogenic fungus *Fusarium oxysporum* Schl. f.sp. *herbemontis* (CAVALCANTI, 2021), using a GC-MS-based metabolomic approach. This work provides a discussion of primary metabolite profiles modulation induced by the early (0 days after the treatment- DAT), medium (4 DAT), and late (8 DAT) fungus co-culture. Thus, the identification of potential markers can be used to monitor or diagnose the disease at different times, as well as to assist helping the bases of breeding programs to reduce the alarming losses of viticulture caused by *Fusarium* around the world.

Material and methods

Figure 1. Experimental procedure

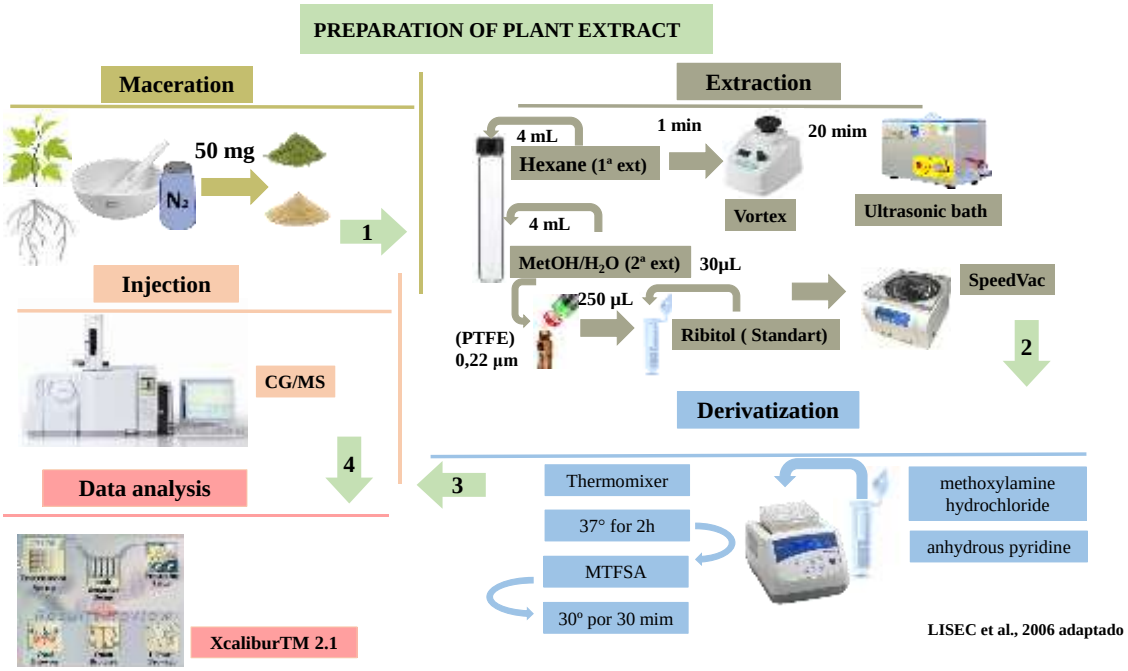

Chemicals

GC-grade n-Hexane and methanol (Merck, Germany, besides ultra pure water were used to extract and obtain polar fractions of analytical interest. Methoxyamine hydrochloride, pyridine and N-methyl-N-(trimethylsilyl) trifluoro-acetamide for gas chromatography (Sigma-Aldrich) were used in the derivatization step. Ribitol was purchased from Sigma-Aldrich (99% purity).

Plant and fungal materials

The biological materials were produced as previously reported (CAVALCANTI, 2021). The seedlings clones were provided by EMBRAPA Uva e Vinho located in Bento Gonçalves (Rio Grande do Sul State, Brazil) corresponding to the following *Vitis* sp. genotypes: BDMG-573 [(Bordô (*Vitis labrusca*) x Magnólia (*Vitis rotundifolia*)] and 'Paulsen' (P1103) [*Vitis berlandieri* x *Vitis rupestris*]. They were grown in culture containing solid Galzy medium until they reached 60-days-old. Approximately 01 cm nodal segments with an axillary bud and a leaf were cut from plants and were cultured tubes containing 12 mL of modified Galzy medium (MURASHIGE; SKOOG, 1962), with 8.0 μmol L^{-1} ANA (naphthaleneacetic acid), 2% sucrose and 0.6% agar, pH 6.1, and autoclaved at 1 atm and 121 °C for 20 minutes. The regenerated seedlings were propagated *in vitro* in duplicates, in culture tubes (11.5 x 2.5 cm) with approximately 5 mL of medium, and kept in a growth chamber at 23 ± 3 °C, under a photoperiod of 16 h with PPFD of 75 μmol photons $m^{-2}.s^{-1}$. After rooting (45 to 60 days), one seedling was transferred into a new Galzy medium tube, under the same conditions described above (Figure S1). The *Fusarium oxysporum* Schl. f.sp. *herbemontis* colonies were established in an agar-based medium for two weeks provided by the Laboratory of Phytopathology of Embrapa Agroindústria Tropical located in Fortaleza (Ceará State, Brazil).

Figure 2. Seedlings clons of *Vitis* in Galzy medium. A) BDMG-573 genotype and B) P1103 genotype.

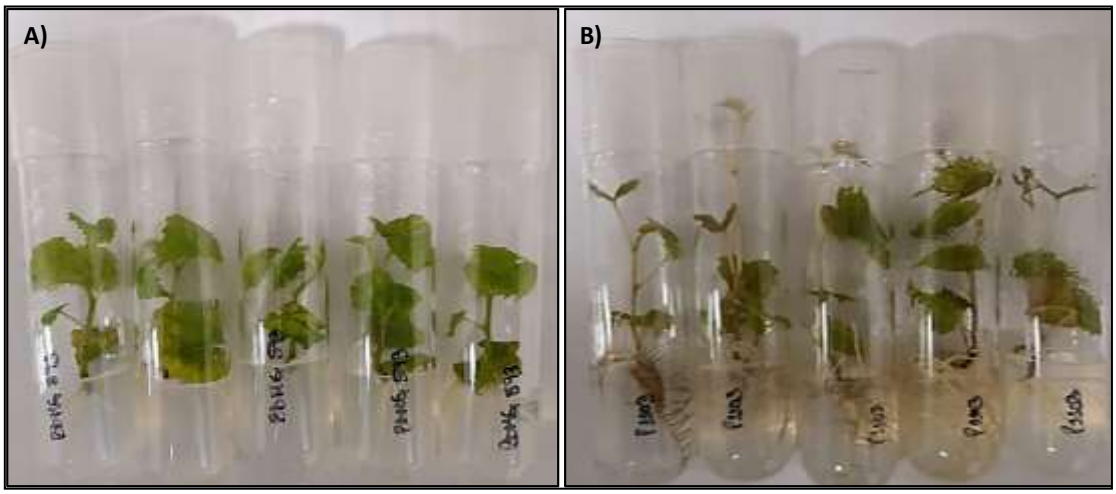

Experimental and co-cultivation conditions and treatments

In vitro co-cultivation was performed in a sterilized laminar flow hood by transferring 30 mm disks of PDA (potato dextrose agar) with fungal mycelia into each tube containing the seedling (20 mm away from the stem) using sterile forceps (CAVALCANTI, 2021). Then, the tubes were closed and sealed with plastic film and incubated in an acclimatized room of the Laboratório Multiusuário de Química de Produtos Naturais from Embrapa Agroindústria Tropical at 25 °C for a 12 h photoperiod. For the control group, the tubes containing the seedlings in Galzy medium were not exposed to any fungus colonies, and kept in the same conditions as the co-cultured group. The seedlings were evaluated at three different days after treatment (DAT) with the fungus: a) day "zero", which was at eight hours after treatment (0 DAT); b) after four days of treatment (4 DAT); and c) after eight days of treatment (8 DAT). The co-cultured and control groups were collected at the times described above. Their roots were separated from the aerial parts and immediately placed in liquid N_2 and stored at -80 ºC in ultra-freezer. Thus, the experiment consisted of two *Vitis* genotypes, BDMG-573 and Paulsen P1103, two treatments (control and co-cultivated) and three harvest times (0, 4, and 8 DAT), comprising four biological replicates.

Plant extract preparation

To obtain the plant extract, aerial part and roots were initially powdered in liquid N_2. Afterwards, 50 mg of each material plant were mixed with 4 mL of hexane, vortexed for 1 minute for homogenization, and placed in an ultrasound bath at 135 W during 20 min. Next, 4 mL of a methanol/water (7:3) solution was added to the mixture, repeating the vortex and ultrasonic bath steps. The solution was centrifuged at 3000 rpm for 10 min, affording two phases (nonpolar and polar supernatant). Finally, 01 mL aliquots of the lower phase (water-methanol) were filtered through hydrophilic Polytetrafluoroethylene (PTFE) 0.22 µm filter, then stored in vials in ultra-freezer (-80ºC) until GC-MS analysis. A 250 µL aliquot of the water-methanol (polar) phase was mixed with 30 µL of the internal standard ribitol (0.2 $mg.mL^{-1}$) and centrifuged at 14000 rpm for 10 min. Later on, an aliquot of 250 µL of the supernatant was transferred to a microtube and dried on a speed vac equipment (SpeedVac Concentrator, Eppendorf, Hamburg, Germany) overnight. Finaly, the metabolites from the dry polar fractions were

derivatized using methoxylamine hydrochloride (20 $mg.mL^{-1}$) in pyridine by shaking at 37 °C for 2 h, followed by addition of N-methyl-N-(trimethylsilyl)-trifluoro acetamide (MSTFA). The reaction mixture was kept under stirring at 37 °C for 30 min and injected in the GC-MS (LISEC et al., 2006).

Gas cromatography and mass spectrometry conditions

The GC-MS analyses were accomplished on a QP-PLUS 2010 Shimadzu GC-MS instrument (Japan). One microliter of the sample was injected in split mode (1:10 ratio) with helium gas as carrier gas at a flow rate of 1.0 $mL.min^{-1}$ in an RTX-5MS capillary column (30 mx 0.25 mm x 0.25 µm) to separate the metabolites. The chromatographic runs were carried out at 80 °C for 5 min, then increased to 310 °C by 8 °C/min and maintained for 1 min at this temperature. The injection, ions source, and MS interface temperatures were 230 °C, 200 °C, and 250 °C, respectively. The mass spectrometer was operated at 70 eV (EI) in a scanning range of 80-700 (m/z), initiated after a solvent cut-off time of 3 min.The chromatograms and mass spectra were processed using the Xcalibur™ 2.1 software (Thermo Fisher Scientific, Waltham, MA, USA). The metabolites were identified based on the comparison of their retention times and fragmentation patterns with an internal MS library composed of metabolite standards and as well with those of Golm's metabolome database Arabidopisis fragmentation patterns (Max Planck Institute of Molecular Plant Physiology) avaliable in http://gmd.mpimp-golm.mpg.de/analysisinput.aspx. The relative value of each metabolite was determined by dividing their respective peak areas by the internal standard ribitol peak area, then divided by the fresh mass of the sample.

Experimental design and statistical analysis

The experimental design consisted of two *Vitis* sp genotypes, two previously explained treatments (control and co-cultured) at three evaluation times (0, 4, and 8 days). For the metabolic analysis, the files were processed on the MetaboAnalyst 5.0 server (http://www.metaboanalyst.ca). The data were normalized by log transformation and automatic scaling that fitted a better statistical normal distribution. The Principal Component Analysis (PCA) was performed to show the differences among the two treatments and analyzed times for each plant tissue, separately. To evaluate the effect of

the treatment concerning the control on the metabolic profile, Orthogonal Partial Least Squares Analysis – Discriminant Analysis (OPLS-DA) and variable importance in projections (VIP scores) were performed for leaves and roots separately for each genotype and times, obtaining the principal discriminating metabolites. The hierarchical heatmaps were built by Euclidean distance based on a one-way analysis of variance (ANOVA).

Results

Metabolic profiles of two *Vitis* sp genotypes at different times

A total of 46 metabolites were identified, of which 22 were amino acids, 7 were organic acids, 15 were carbohydrates, and 2 were other classes (Table 1) based on Kyoto Encyclopedia of Genes and Genomes (KEGG ID). A total of 45 metabolites were found in shoots of both genotypes, and 46 were found in the roots, which β-Alanine was included.

Table 1: List of metabolites detected in the both BDMG573 and P1103, as well as roots and shoots. The names and compound IDs were based on Kyoto Encyclopedia of Genes and Genomes (KEGG ID). *β-alanine was found only in roots.

Number	Metabolite	Compound type	Retention Time (min)	Compound id
1	Lactic acid	Organic acid	7.38	C00186
2	Alanine	Amino acids	8.43	C00041
3	1,3-Dihydroxyaceton	Carbohydrates	10.23	C00184
4	Valine	Amino acids	11.01	C00183
5	Urea	Others	11.43	C00086
6	Serine	Amino acids	11.83	C00065
7	Leucine	Amino acids	12.15	C01933
8	Phosphoric acid	Organic acid	12.23	C00009
9	Glycerol	Carbohydrates	12.24	C00116
10	Isoleucine	Amino acids	12.57	C00407
11	Proline	Amino acids	12.61	C00148
12	Glycine	Amino acids	12.81	C00037
13	Glyceric acid	Organic acid	13.32	C00258
14	Fumaric acid	Organic acid	13.49	C00122
15	Maleic acid	Organic acid	13.51	C01384
16	Threonine	Amino acids	14.33	C00188
17	β-Alanine *	Amino acids	14.93	C00099
18	Malic acid	Organic acid	16.02	C00149
19	Methionine	Amino acids	16.46	C00073
20	Aspartic acid	Amino acids	16.51	C00049
21	4-hydroxy-proline	Amino acids	16.61	C03651
22	N-acetyl-Serine	Amino acids	17.63	C00979
23	Asparagine	Amino acids	17.88	C00152
24	Glutamic acid	Amino acids	17.98	C00025
25	Phenylalanine	Amino acids	18.11	C00079
26	Xylose	Carbohydrates	18.71	C00181
27	Arabinose	Carbohydrates	18.77	C00216
28	Ribose	Carbohydrates	19.01	C00121
29	Glutamine	Amino acids	20.16	C00064
30	Ornithine	Amino acids	20.76	C00077
31	Citric acid	Organic acid	20.85	C00158
32	Adenine	Others	21.41	C00147
33	Fructose	Carbohydrates	21.77	C02336
34	Mannose	Carbohydrates	21.82	C00159
35	Glucose	Carbohydrates	21.98	C00031
36	Lysine	Amino acids	22.06	C00047
37	N2-acetyl-Ornithine	Amino acids	22.07	C00437
38	Histidine	Amino acids	22.12	C00135
39	Galactose	Carbohydrates	22.18	C00124
40	Tyrosine	Amino acids	22.3	C00082
41	Sorbitol	Carbohydrates	22.37	C00794
42	Glucuronic acid	Carbohydrates	22.48	C16245
43	Inositol myo	Carbohydrates	24.28	C00137
44	Sucrose	Carbohydrates	30.03	C00089
45	Cellobiose	Carbohydrates	30.98	C06422
46	Maltose	Carbohydrates	31.27	C00208

To evaluate differences between control non-co-cultivated (CNT) and co-cultivated with the *Fusarium oxysporum* (FUS) of both genotypes at days after treatment (0 DAT, 4 DAT, and 8 DAT), we performed multivariate analyses of principal component (PC) of the GC-MS dataset from shoots and roots, separately. Considering shoot, at 0 DAT, the PC1 and PC2 accounted for 44.2% and 21.8% of the total variation, respectively (Figure 3A). The plot showed a complete separation of P1103_FUS from the other treatments mainly by PC1 component. On the other hand, there was a complete overlap between BDMG573_CNT and BDMG573_FUS, indicating similar metabolic profiles, besides overlapping between the confidence intervals of BDMG573_FUS and P1103_CNT. The top four most positive contributions were aspartic acid, citric acid, glutamine, and glyceric acid to PC1 (Figure 3B). All metabolite contributions have been provided in supplementary table S2. At 4 DAT, the PC1 and PC2 accounted for 41.5% and 17.9% of the total variation, respectively (Figure 3C). The scores plot exhibited a clear separation among the four treatments. The top four metabolites that contributed to groups separation were threonine, citric acid, glyceric acid, and malic acid, for PC1, and sucrose, myo-inositol, histidine, and glutamine for PC2 (Figure 3D, and Table S2). At 8 DAT, the PC1 and PC2 accounted for 35.2% and 23.2% of variation, respectively (Figure 3E). There was a well-done separation between BDMG573 and P1103, independent of the treatment by the PC1 axis. Although there was a broad distribution of BDMG573_FUS over the plot, it overlapped the BDMG573_CNT, as well as the P1103_CNT confidence interval overlapped P1103_FUS. The top four metabolites that contributed to groups discrimination were aspartic acid, glycine, sorbitol, and maltose, for PC1, followed by phosphoric acid, lysine, ornithine, and N2-acetyl-ornithine for PC2 (Figure 3F).

Figure 3 - Two-dimensional principal component analysis (PCA) of shoot metabolic profiles of two *Vitis* genotypes BDMG-573 and P1103. The plants were co-cultivated with *Fusarium oxysporum* (FUS) or non-co-cultivated (CNT) and evaluated at 8 hours or 0 DAT (A), 4 DAT (C), and 8 DAT (E). DAT means days after treatment. The loading plots indicate each metabolite contribution for distribution of groups a 0 DAT (B), 4 DAT (D), and 8 DAT (F). Arrows indicated the most top four positive metabolites that were named. The ellipses indicate a 95% confidence interval of the group.

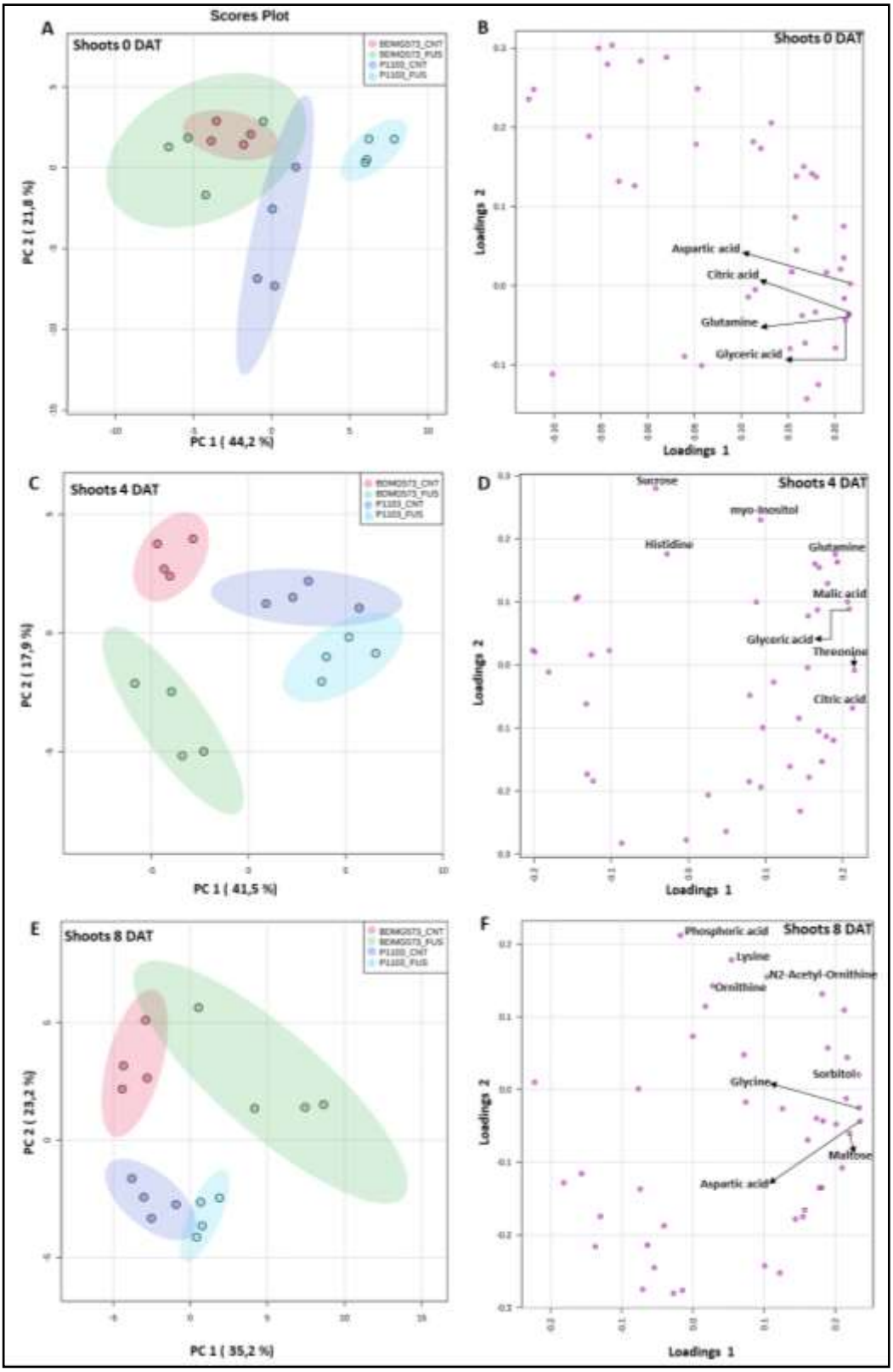

Similarly, multivariate PCAs evaluated roots metabolites of both genotypes covering each time. At 0 DAT, PC1 and PC2 accounted for 47.5% and 18.4% of the total variation, respectively (Figure 4A). The PCA plots exhibited a well-done separation between BDMG573 and P1103 genotypes by PC1 axis. However, there are overlaps between BDMG573_CNT and BDMG_FUS, as well as between P1103_CNT and P1103_FUS, which indicates a similar metabolic profiles of each genotype under CNT and FUS treatments. The top four most positive contributions were mannose, malic acid, cellobiose, and glucose for PC1, followed by glycine, serine, leucine, and isoleucine for PC2 (Figura 4B, and Table S2). At 4 DAT, the PC1 and PC2 accounted for 48.2% and 22.9% of the total variation, respectively (Figure 4C). The plot exhibited well-done separation between BDMG573 and P1103 genotypes and between BDMG573_CNT and BDMG573_FUS treatments, indicating a higher variation of BDMG573 than at DAT0. On the other hand, there was an overlap between P1103 treatments as noticed at 0 DAT. The top four metabolites that contributed to groups separation were malic acid, sorbitol, mannose, and glyceric acid, for PC1, and sucrose, phenylalanine, Glucose, and N- acetyl-serine (Figure 4D, amd Table S2). At 8 DAT, the PC1 and PC2 accounted for 38.3% and 29.5% of the variation, respectively (Figure 4E). There was a well-done separation between BDMG573_CNT and P1103_CNT, as well they were separated from their respective FUS treatment. On the other hand, the profile of BDMG573_FUS overlapped P1103_FUS. The top four metabolites that contributed to groups discrimination were sorbitol, ribose, urea, and cellobiose, for PC1, followed by adenine, methionine, fumaric acid, and aspartic acid for PC2 (Figure 4F, and Table S2).

Figure 4 - Two-dimensional principal component analysis (PCA) of roots metabolic profiles of two *Vitis* genotypes BDMG-573 and P1103. The plants were co-cultivated with *Fusarium oxysporum* (FUS) or non-co-cultivated (CNT) and evaluated at 8 hours or 0 DAT (A), 4 DAT (C), and 8 DAT (E). DAT means days after treatment. The loading plots indicate each metabolite contribution for distribution of groups a 0 DAT (B), 4 DAT (D), and 8 DAT (F). Arrows indicated the most top four positive metabolites that were named. The ellipses indicate a 95% confidence interval of the group.

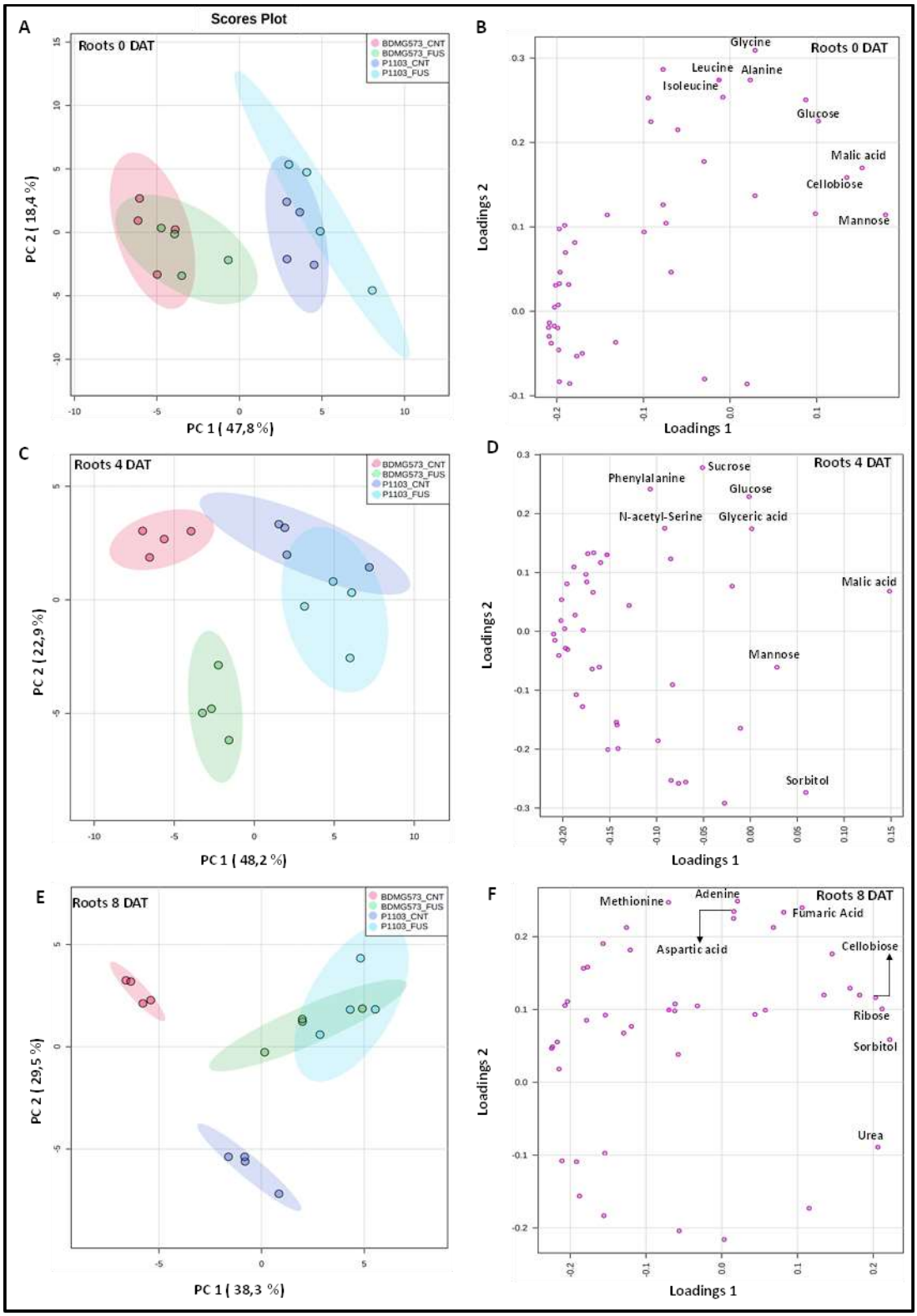

Significative metabolite modulation in *Vitis sp* induced by early, medium and late fungus co-cultive

Heat maps overview detailing the positive or negative modulation of metabolites in were generated comprising the two genotypes (BDMG573 and P1103) on each treatment separately by DAT, similarly to PCA. The metabolites with statistical differences ($p<0.05$) were marked between the comparisons: BDMG573_CNT/BDMG573_FUS, P1103_CNT/P1103_FUS, as well as BDMG573_CNT/P1103_CNT, and BDMG573_FUS/P1103_FUS. The analysis of shoots heatmaps showed a division of FUS and CNT treatments in the BDMG573 genotype at times 0 and 4 DAT. While in the P1103 genotype, it occurred at 4 and 8 DAT (Figure 5). At 0 DAT, only two metabolites (4-hydroxyproline and threonine) were significantly different between BDMG573_FUS and CNT. However, 21 metabolites were statistically significant in the P1103_FUS compared to the control, most of which had a positive modulation. Comparing different genotypes and same treatment, 15 and 25 metabolites were significant between treatments BDMG573_CNT and P1103_CNT and BDMG573_FUS and P1103_FUS (Figure 5A). At 4 DAT, there were 15 metabolites significantly modulated between BDMG573_FUS and CNT, positively and negatively, whereas only 07 metabolites were significant in P1103_FUS compared to the control. Comparing different genotypes, 21 and 22 metabolites were different in the same treatment treatments BDMG573_CNT and P1103_CNT and BDMG573_FUS and P1103_FUS (Figure 5B). At 8 DAT, there were 20 metabolites significantly modulated between BDMG573_FUS and CNT (05 increased, and 15 decreased), whereas only 05 metabolites were significantly increased in P1103_FUS compared to control. Comparing different genotypes, 12 and 20 metabolites were significant between treatments BDMG573_CNT and P1103_CNT and BDMG573_FUS and P1103_FUS (Figure 5C).

Figura 5 - Hierarchical heat maps grouped by Euclidean distance of shoots genotypes P1103 and BDMG573 at different times of co-culture with *Fusarium oxysporum* (FUS), as well as the control non-co-cultured (CNT). A) 0 DAT; B) 4 DAT and C) 8 DAT (days after treatment). The squares represent the log_2 mean of four replicates, and the color map shows an increase (red scale) or decrease (blue scale) of each metabolite. Asterisks (*) indicate significant diference by anova ($p<0.05$) between treatments within same genotype (BDMG573_FUS x BDMG573_CNT or P1103_FUS x P1103_CNT). Hashtag (#) indicate significant difference between genotypes within same treament (BDMG573_FUS x P1103_FUS or BDMG573_CNT x P1103_CNT)

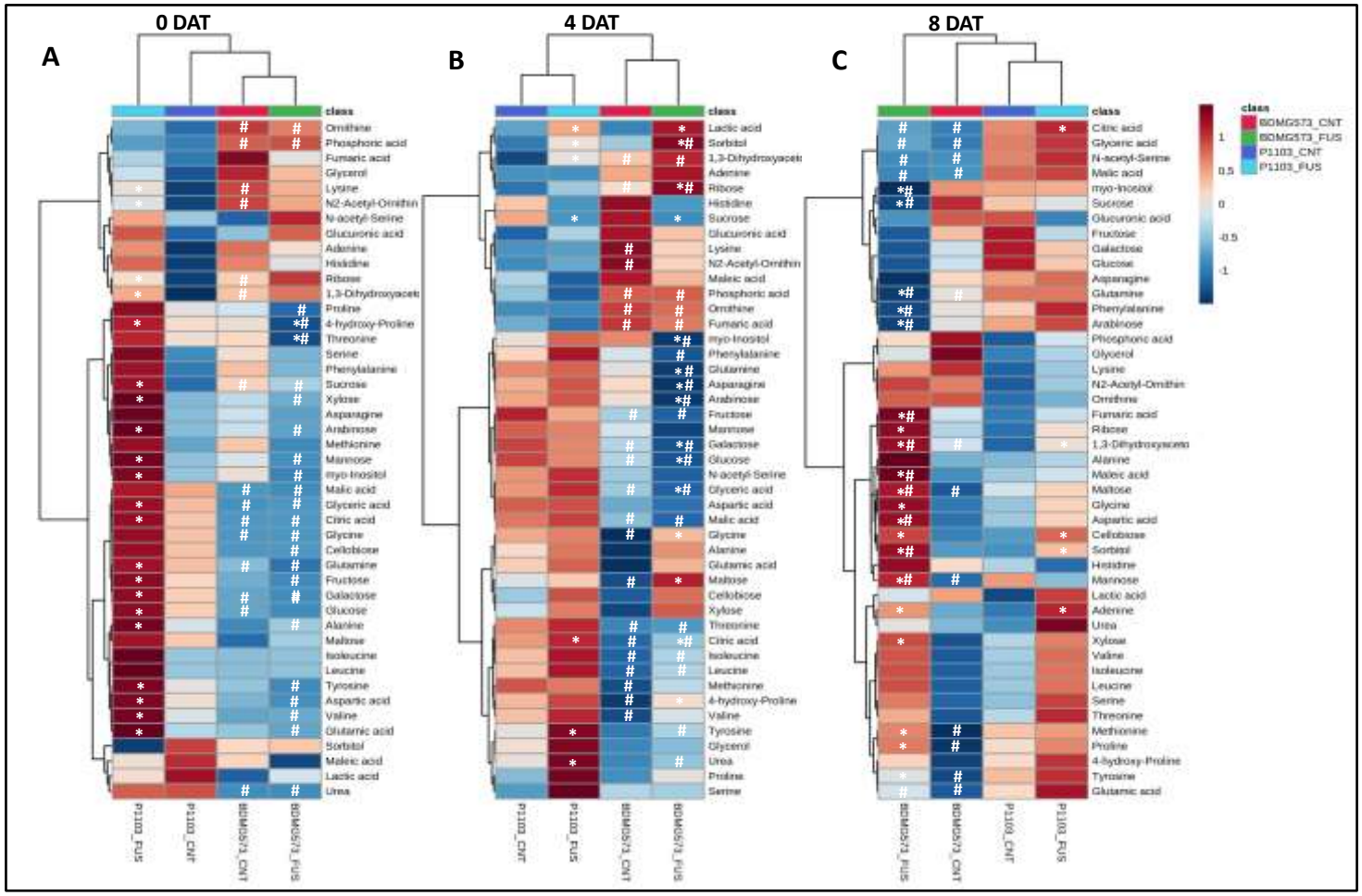

Regarding the heatmaps of roots, there are six (five increased and one decreased) metabolites statistically different in BDMG573_FUS and three (one increased and three decreased) metabolites in the P1103_FUS when compared to their control treatments, at 0 DAT (Figure 6A). Overall, the heatmap showed several metabolites higher in the BDMG genotype. Twenty-four and 25 metabolites were differentially modulated when comparing the two genotypes in each treatment, respectively BDMG573_CNT x P1103_CNT and BDMG573_FUS x P1103_FUS (Figure 6A). At 4 DAT, 28 and 16 were significantly modulated in the genotypes BDMG573_FUS and P1103_FUS, respectively. Among them, there are a large number of amino acids decreased in both genotypes, although some sugars were increased while others were also decreased. While 31 and 30 metabolites were differentially modulated when comparing the genotypes in each treatment, respectively BDMG573_CNT x P1103_CNT and BDMG573_FUS x P1103_FUS. At 8 DAT, there were 32 (seven were the most positive highlighting alanine, cellobiose, and 1,3-dihydroxyacetone) and 26 metabolites were significantly modulated in genotypes BDMG573_FUS and P1103_FUS, respectively. On the other hand, 17 and 23 metabolites were statistically different when comparing BDMG573_CNT x P1103_CNT and BDMG573_FUS x P1103_FUS, respectively.

Figure 6 - Hierarchical heat maps grouped by Euclidean distance of shoots genotypes P1103 and BDMG573 at different times of co-culture with *Fusarium oxysporum* (FUS), as well as the control non-co-cultured (CNT). A) 0 DAT; B) 4 DAT and C) 8 DAT (days after treatment). The squares represent the log_2 mean of four replicates, and the color map shows an increase (red scale) or decrease (blue scale) of each metabolite. Asterisks (*) indicate significant diference by anova ($p<0.05$) between treatments within same genotype (BDMG573_FUS x BDMG573_CNT or P1103_FUS x P1103_CNT). Hashtag (#) indicate significant difference between genotypes within same treament (BDMG573_FUS x P1103_FUS or BDMG573_CNT x P1103_CNT)

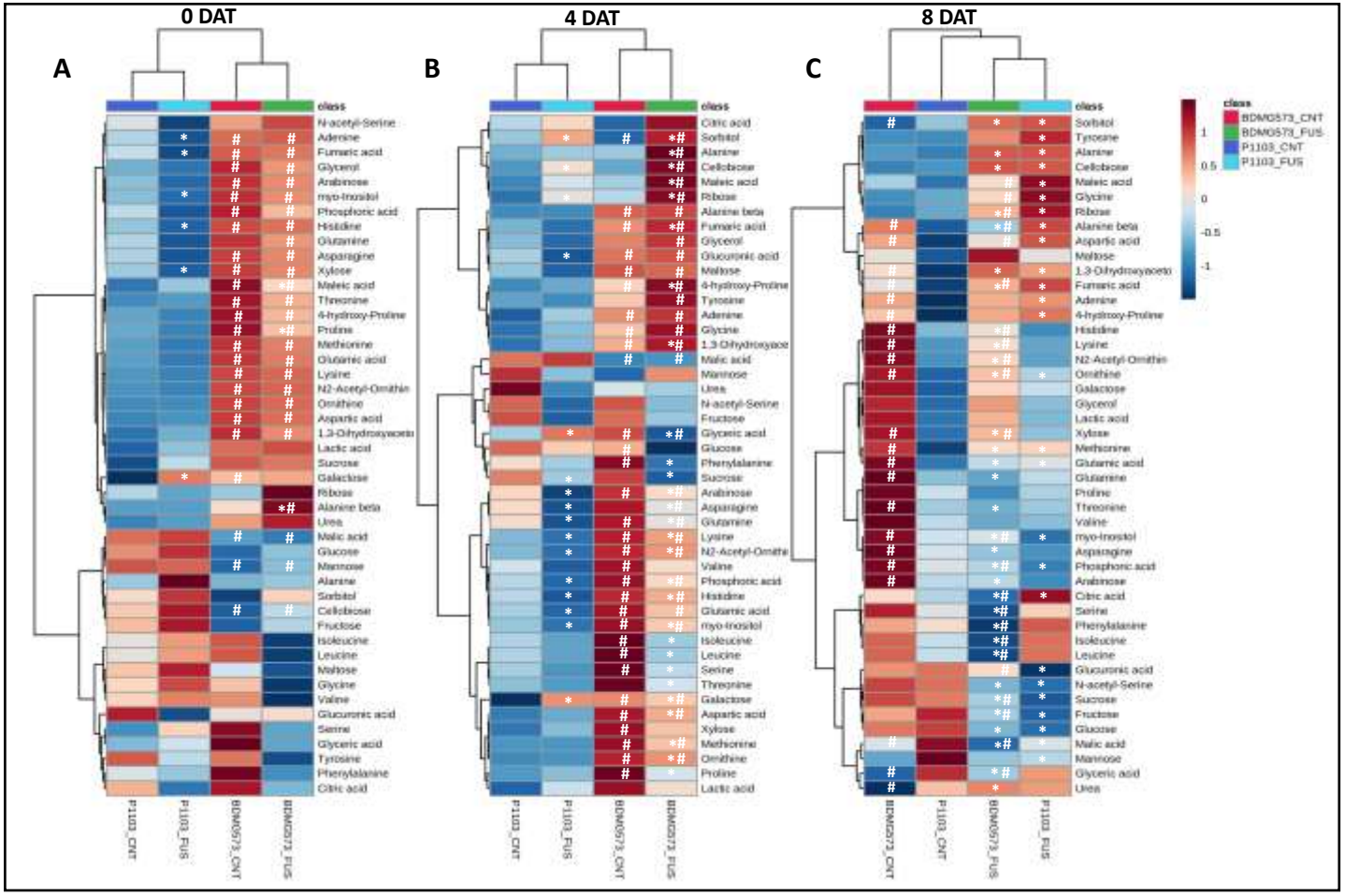

Identification of potential biomarkers in Vitis sp genotypes after *F. oxysporum* co-cultivation

Orthogonal Partial Least Squares-Discriminant Analysis (OPLS-DA) exhibited the positive and negative potential biomarkers of each *Vitis* genotypes co-cultivated with *F. oxysporum* at three different times. The variable importance in projections (VIP scores) with VIP >1.0 were based in the values of orthogolnal components 1 and 2 (Figure S1 and Figure S2). However, we explore the S-plot since it combines the major contribution of probalility and correlation ranked from the highest to the lowest reliability values using the respective control treatment (non-co-cultivated) as reference. Analyzing the shoots of BDMG573_FUS compared to the control treatment, at 0 DAT, the top three positive metabolites were ribose, 1,3-dihydroxyacetone, and glucoronic acid, and 4-hydroxy-proline was the most negative (Figure 7A). At 4 DAT, the three positive metabolites were lactic acid, 1,3-dihydroxyacetone, and maltose, and glutamine was the most negative (Figura 7B). At 8 DAT, the three positive metabolites were mannose, sorbitol, and maltose, and myo-inositol was the most negative (Figure 7C). The same was performed for shoots of P1103 _FUS compared to the control treatment. At 0 DAT, the top three positive metabolites were glyceric, malic, and citric, and the sugar sorbitol had the most negative influence (Figure 7D). At 4 DAT, the three positive discriminant metabolites were proline, serine, and tyrosine, and sucrose had the most negative impact (Figura 7E). At 8 DAT, the three positive metabolites were sorbitol, cellobiose, and urea, and fructose was the most negative (Figure 7F).

In the roots of BDMG573_FUS compared to the control treatment, at 0 DAT, the top three positive discriminant metabolites were β-alanine, mannose, and citric acid, and 4-hydroxy-proline was the most negative (Figure 8A). At 4 DAT, the three most positive metabolites were cellobiose, sorbitol, and alanine, and phenylalanine was the most negative (Figura 8B). At 8 DAT, the three most positive metabolites were urea, cellobiose, and sorbitol, and phosphoric acid was the most negative (Figure 8C). Similarly, in the roots of P1103_FUS compared to the control treatment, at 0 DAT, the most positive discriminant metabolites were galactose, maleic acid and alanine, and glucoronic acid was the most negative (Figure 8D). At 4 DAT, the three most positive metabolites were the sugars galactose, sorbitol and cellobiose, and arabinose was the most negative (Figura 8E). At 8 DAT, the three most positive metabolites were 1,3-dihydroxyacetone, adenine, and ribose, and sucrose was the most negative (Figure 8F).

Figure 7 - S-plots from Orthogonal Projections to Latent Structures Discriminant Analysis (OPLS-DA) shoots of vitis genotypes BDMG573 (A, B, and C) and P1103 (D, E, and F) co-cultured with *Fusarium oxysporum* fungus (FUS) compared to non-co-culitvated (CNT). The 3 main significant metabolites that had the major contribution to FUS (upper right corner) and CNT seedlings (lower left corner) were highlighted and their relative content were provided on the right of each plot.

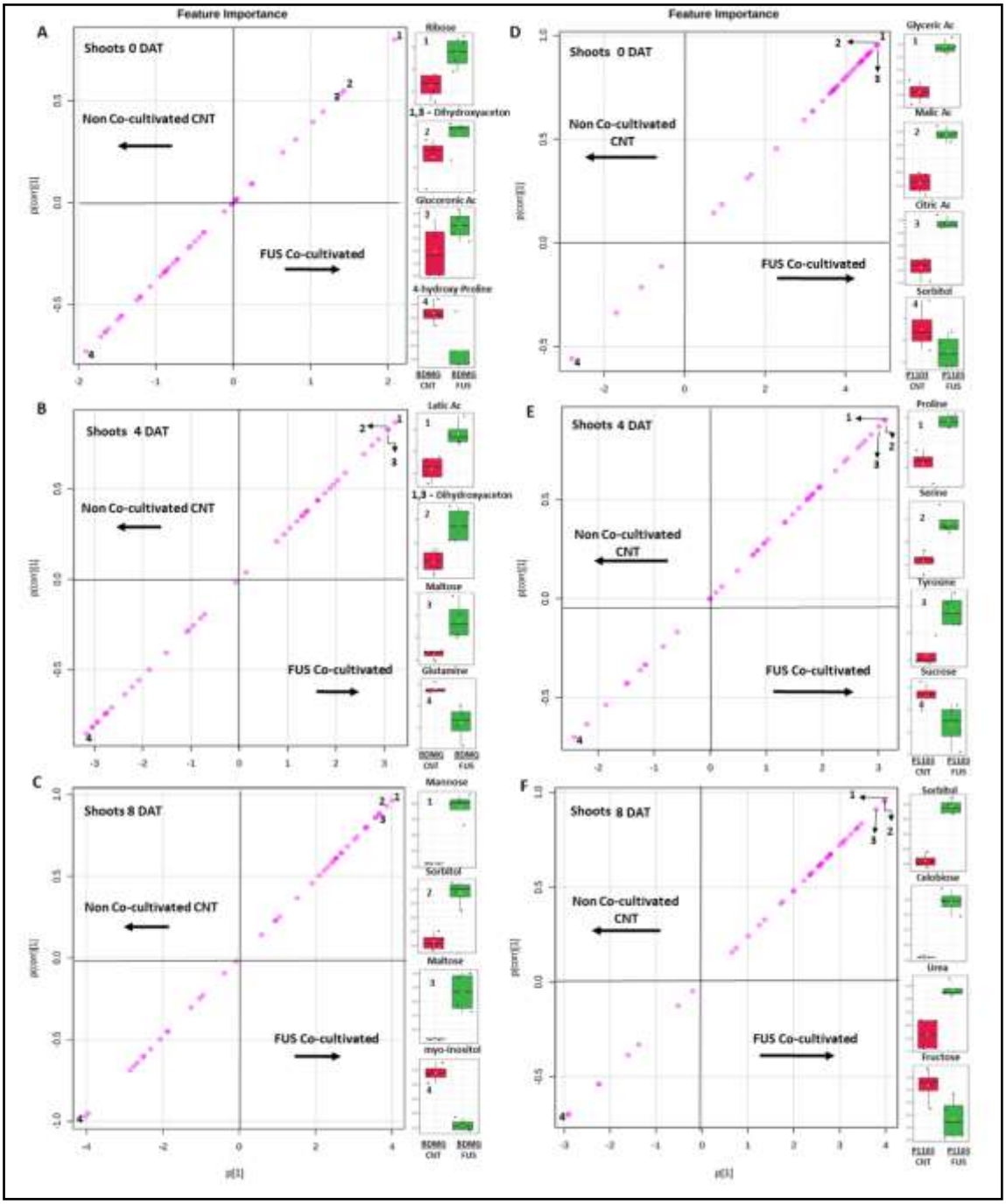

Figure 8 - S-plots from Orthogonal Projections to Latent Structures Discriminant Analysis (OPLS-DA) shoots of Vitis genotypes BDMG573 (A, B, and C) and P1103 (D, E, and F) co-cultured with *Fusarium oxysporum* fungus (FUS) compared to non-co-cultivated (CNT). The 3 most significant metabolites that had the major contribution to FUS (upper right corner) and CNT seedlings (lower left corner) were highlighted and their relative content were provided on the right of each plot.

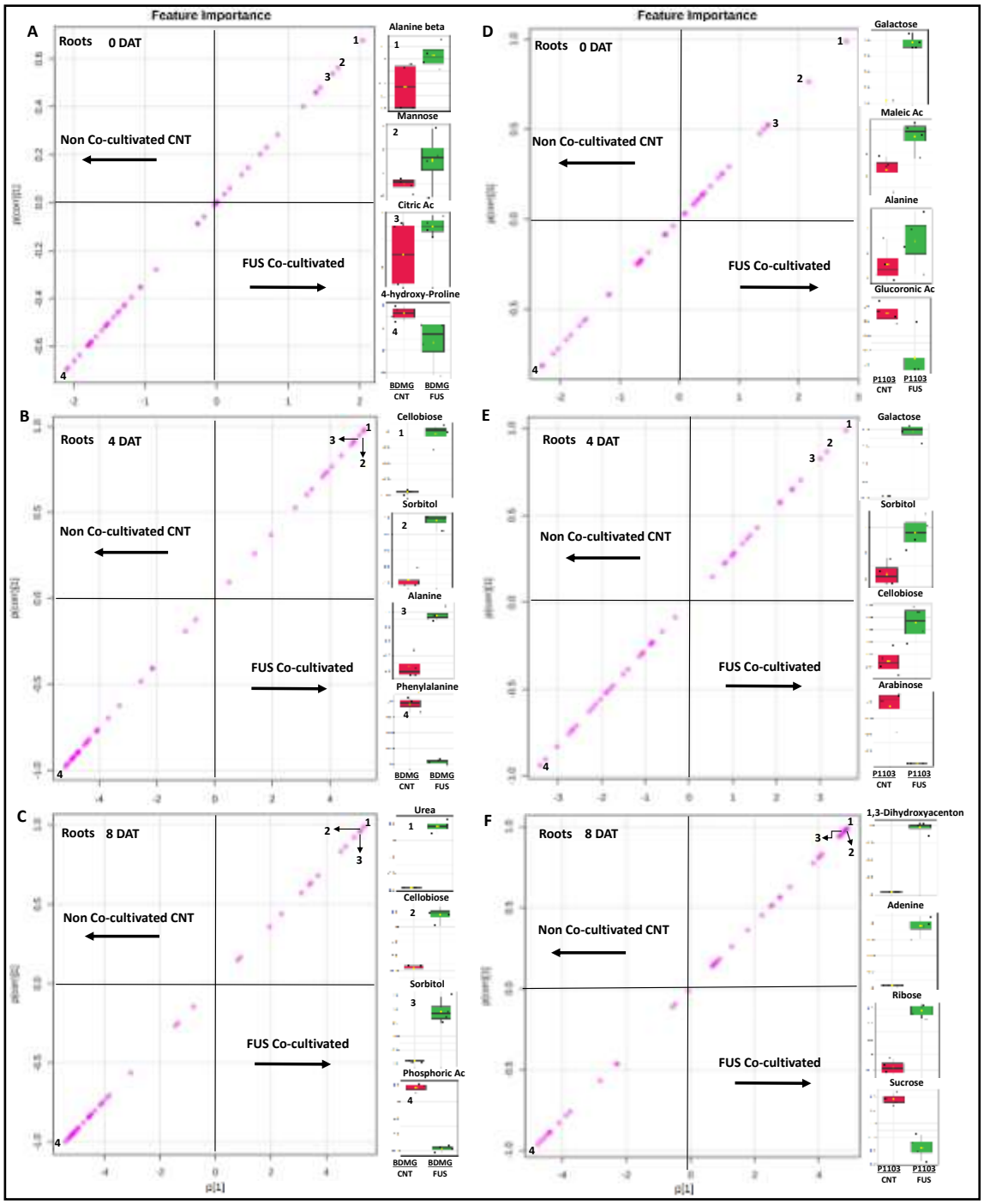

Differential metabolite modulation of BDMG573 and P1103 induced by fungal co-cultivation overtime

The heatmap of the metabolite's relative abundances of shoots and roots provided an overview of the modulation comparing treatments, genotypes, and different exposure times (Figure 9). In the shoots, two main branches diverged the genotypes BDMG573 and P1103 (Figura 9A). Regarding the P1103 treatments, there is a branch comprising the co-cultivated and the control groups at 4 and 8 DAT in which several metabolites were increased, particularly in the co-cultivated treatments. P1103_CNT0 was located more distant from the others. Regarding the BDMG573 treatments, the controls of the three times and BDMG573_FUS0 were placed in the same main branch, in which it was possible to note a tendency of the decreasing of several metabolites. On the other hand, there is a branch comprising BDMG573_FUS4 and BDMG573_FUS8, in which there is a tendency of increasing several metabolites at 8 DAT .

In the roots, two main branches diverged the genotypes BDMG573 and P1103, except by P1103_FUS8 which was close to BDMG573_FUS4 and DMG573_FUS8 (Figura 9B). In general, there was a similar overview of P1103 treatments, in which there was a tendency to decrease the majority of metabolites in relation to BDMG573. On the other hand, two branches separated BDMG573, one comprising control treatments at 0, 4, and 8 DAT, and BDMG573_FUS0, in which there is an increase of several metabolites. The other one comprised BDMG573_FUS4, BDMG573_FUS8, and P1103_FUS8, which presented a tendency to increase several others metabolites.

Figure 9- Hierarchical heat maps grouped by Euclidean distance of shoots (A) and roots (B) metabolites of the two varieties of *Vitis* sp BDMG573 and P1103. Each square represents the log2 mean of four replicates, and the color map shows an increase (red scale) or decrease (blue scale) of each metabolite compared to the control and co-cultivated plants for each time point (0, 4, and 8 DAT).

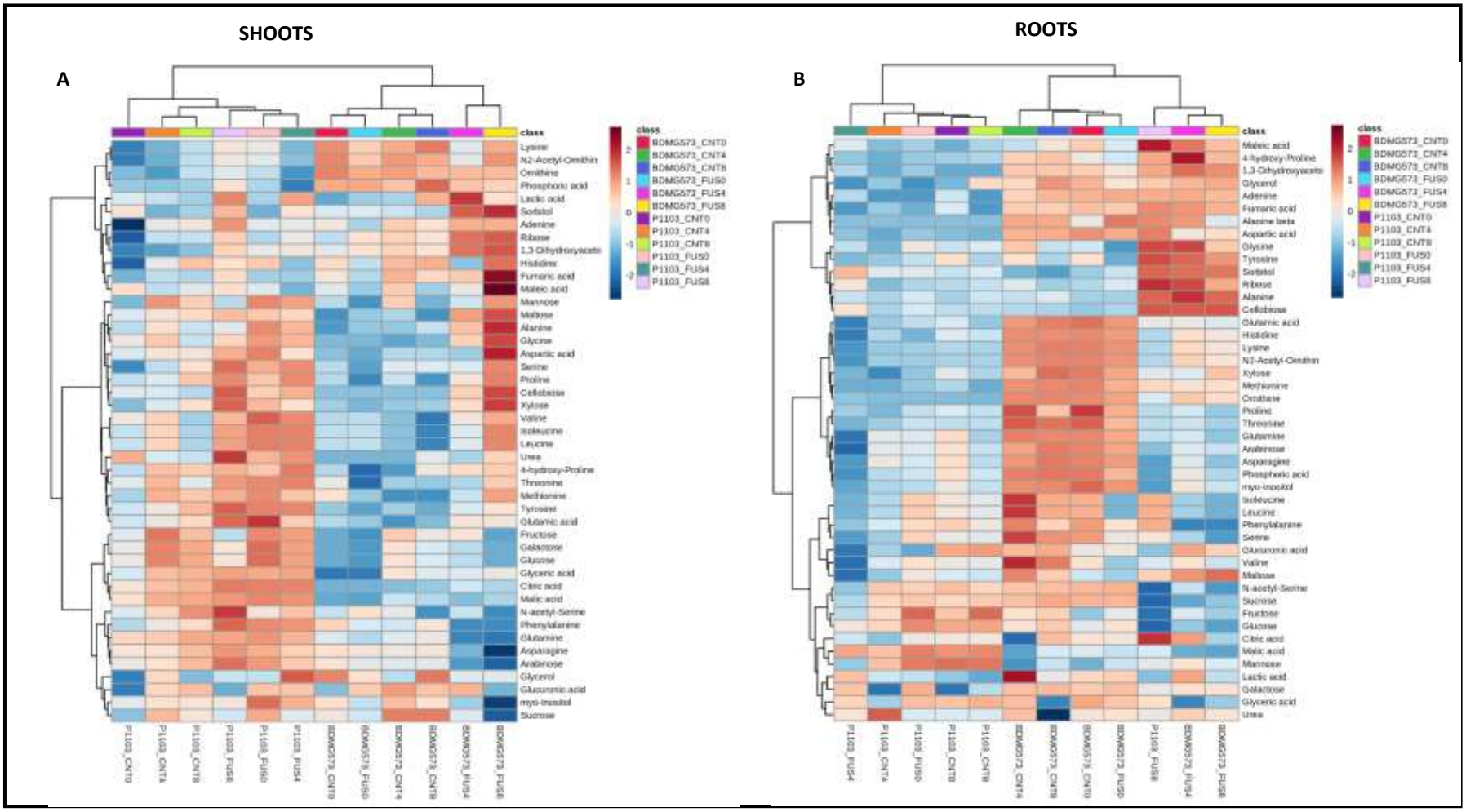

Discussion

The *Vitis* genotypes co-cultivated with *Fusarium oxysporum* (FO) show different metabolic profiles

Changes in primary metabolism in vines occur in response to stressful conditions, whether biotic or abiotic factors (HARB et al., 2015; FIGUEIREDO et al., 2008). Metabolomics has provided relevant information that helps to understand the biochemistry of the molecular responses of plant-pathogen interaction (CHEN; MA; CHEN, 2019; XU et al., 2015). A multivariate approach evaluated the primary metabolites identified in the shoots and roots of the BDMG573 and P1103 *Vitis* genotypes co-cultured in vitro with the Fo fungus. Principal component analysis (PCA) showed different patterns in which the metabolic profiles varied for each time, genotype, and plant organ, differences were clear in the heatmap (Figure 9). Similarly, in watermelon infected with Fo, the metabolic profiles were genotype specific and distinct in leaves and roots (KASOTE et al., 2020). In the current study, the different treatments non-co-cultured (CNT) and co-cultured with the fungus (FUS) resulted in different metabolic profiles (Figures 3 and 4) and significant alterations in the modulation of amino acids, carbohydrates, organic acids, and other metabolites for each *Vitis* genotype are highlighted through the heat map overview (Figure 5 and 6). Considering an earlier time of co-culture (0 DAT), the overlapping between the metabolic profiles areas of BDMG573_CNT and BDMG573_FUS demonstrate similar metabolic behavior in the first hours of co-culture. On the other hand, the metabolic profile of P1103_FUS was completely separated from the others. In which, there is even a remarkable positive regulation of metabolites (Figure 7A). It indicates a quick change of metabolites that may be related to the tolerance process described for this genotype (VILVERT et al., 2017). However, at 4 DAT, the treatments of the BDMG573 genotype separate (Figure 1C) is showing a distinct behavior from P1103, confirmed by the lower modulation of some metabolites such as citric acid, glutamine, and glyceric acid. Also, BDMG573_FUS compared to CNT showed two different groups of positive and negative metabolites. For P1103, a slight overlapping indicates similar metabolic profiles of CNT and FUS, which a remarkable modulation of citric acid, tyrosine, and urea (Figure 7B). These slight overlaps between treatments in the same genotype persist at 8 DAT. However, there is a greater amplitude of the BDMG573_FUS area (Figure 3E), which we can infer

balance positively and negatively modulated metabolites (Figure 7C). In the P1103 genotype, the metabolic profiles of the two treatments are closer (Figure 3E), once there is remarkable positive modulation of citric acid, added by others such as adenine, cellobiose, and sorbitol (Figure 7C). This close relation that P1103 treatments became over time suggest some tolerance associated to the tendency of positive regulation in FUS treatment, as P1103 has demonstrate tolerence to biotic and abiotic stresses (DALDOUL et al., 2020).

Overall, roots showed more differences in metabolic modulation between CNT and FUS treatments, probably because they were first exposed to *F. oxysporum* (Figure 4). Indeed, there are a variety of specific responses in roots to pathogens that remains unclear (CHUBERRE et al., 2018). PCA of 0 DAT showed similar behavior concerning overlapping areas (Figure 4 A) and a little metabolic differentiation between the CNT and FUS groups of the two genotypes (Figure 8A). Otherwise, at 4 DAT, the treatments BDMG573_CNT and BDMG573_FUS (Figure 4 C) showed considerable separation of profiles and the metabolic modulation of the plant in response to the fungus attack that was clear in the heat map (Figure 8 B). At the same time, the CNT and FUS analysis groups of the P1103 genotype both demonstrate considerable overlapping of areas (Figure 4C) denoting low metabolic modulation of the plant by infection (Figure 6B), which is consistent with the better performance under fungus co-cultivate (CAVALCANTI, 2021; DALDOUL et al., 2020; MORSCH et al., 2021). Finally, in the 8 DAT roots (Figure 4 E), the BDMG573_CNT and BDMG_FUS groups showed complete separation of their component plots, as well as P1103_CNT and P1103_FUS. However, the FUS treatments of the two genotypes overlapped. In the heat maps (Figure 6 C), the metabolic modulation between groups BDMG_CNT8, BDMG_FUS8, and P1103_FUS8. Therefore, it can be inferred that the roots of both genotypes have responses to the pathogen attack, which indicates the presence of plant-pathogen interaction (WONG et al., 2020).

Identification of potential biomarkers in the BDMG573 and P1103 genotyes at early, medium and late *Fusarium* co-cultive

The Ortho-PLSDA models for shoots of both genotypes provided the metabolites with the highest discriminating potential, as well as the metabolite with the lowest discriminating potential (Figure 5). In the co-cultured BDMG 573 genotype (Figure 7A and 7B), the sugars ribose and 1,3-dihydroxyacetone and maltose (at 4 DAT), and maltose, sorbitol, and mannose (at 8 DAT). Indeed, the increase of carbohydrates has been related to the maintenance of energy metabolism and defense, which uses these metabolites as a source of carbon skeletons for several biochemical processes, including TCA components for energy production (IGAMBERDIEV; EPRINTSEV, 2016). Maltose is well reported in studies that its presence is indicative of osmotic (DARKO et al., 2019) and saline stress (SHELDEN et al., 2016), leading us to indicate this sugar as a potential biomarker of abiotic and abiotic stresses and the presence of the pathogen in the plant (LEI et al., 2016).

Then, in the first co-cultivation time (0 DAT), shoots of the P1103 genotype presented organic acids (glyceric acid, malic acid, and citric acid) as biomarkers (Figure 7D). It is directly related to TCA to obtain energy that has great importance in the metabolic cycle of the plant (IGAMBERDIEV; EPRINTSEV, 2016). Malic acid and citric acid have their presence reported to tolerance resistance to abiotic stresses, such as aluminum in soybean (SUN et al., 2019; ZHOU et al., 2018) and glyceric acid related to resistance to water stress (LI et al., 2019). On the other hand, in the 4 DAT of P1103_FUS (Figure 7E), the amino acids proline, serine, and tyrosine were the main discriminants for *Fusarium* co-culture. Indeed the presence of the pathogen in the plant drives organic acids from the TCA cycle to the synthesis of amino acids (IGAMBERDIEV; EPRINTSEV, 2016). Thus, proline, serine, and tyrosine are reported to increase in situations of biotic stress and could be used as sources for the production of secondary defense metabolites (TEIXEIRA et al., 2014). Also, proline can act as an energy source, antioxidant, and osmoprotectant to hold stress conditions (CASTELLARIN et al., 2007). For the latest day of P1103_FUS co-culture (8 DAT), the discriminating metabolites were sorbitol, cellobiose, and urea (Figure 7F). The increased presence of carbohydrates is critical to stress response since it stabilizes proteins and protects cellular structures, such as membranes, when stress becomes severe or persists for prolonged periods (THALMANN et al., 2016). As for the presence of urea, it seems to

be related to the protein nitrogen released through catabolic reactions, the amino acids released from protein catabolization are in turn catabolized, leading to the accumulation of ammonium and urea (BEIER; KOJIMA, 2021; WITTE, 2011).

On the other hand, for roots of the BDMG573_FUS genotype at 0 DAT, the most discriminating metabolites were β-alanine, mannose, and citric acid. In the case of β-alanine, studies show the relationship of its synthesis involved with the synthesis of antimicrobial compounds (PARTHASARATHY; SAVKA; HUDSON, 2019). Regarding mannose, it is associated with defense proteins against pathogens (DOS SANTOS SILVA et al., 2019). As the most negative discriminant, 4-hydroxy-proline stands out, an important component that reinforces against cell wall damage (SIDDAPPA; MARATHE, 2020), which may be one of the indications of the root degradation by fungal enzymes (CHEN et al., 2019). Then, the roots of BDMG573_FUS at 4 DAT, and 8 DAT, presented the cellobiose and sorbitol sugars among the main discriminants for both times (Figure 8B and 8C). In which, they are related to stress resistance and signaling for the presence of disease (MENG et al., 2018; ROLLAND; MOORE; SHEEN, 2002). Further, the use of sugars in the roots is related to the low presence of nitrogen (ZHAO et al., 2020). Thus, the presence of urea in the BDMG_FUS of 8 DAT (Figure 8C) makes sense under prolonged biotic stress, occurring due to the high protein degradation as a nutritional source and defense signaling (BEIER; KOJIMA, 2021; GONÇALVES et al., 2020). Therefore, Ortho-PLSDA of the P1103 roots genotype revealed that carbohydrates were the group that showed discriminating metabolites. It is a common fact since these compounds are strictly related to plant growth and development, providing carbon skeletons as a source of energy (LASTDRAGER; HANSON; SMEEKENS, 2014). In addition, they act as signaling molecules in response to stress, helping the plant survive, as discussed before (EVELAND; JACKSON, 2012). At 0 DAT (Figure 8D), and 6 DAT (Figure 8E), the galactose sugar was the metabolite as potential biomarkers, and the 1,3-dihydroxyacetone sugar was for 8 DAT (Figure 8F). It reinforces the presence of sugars in P1103 roots help to maintain tolerance, which involves the integrity of the cell wall, high energy source, and signaling in the presence of the fungus co-culture (IGAMBERDIEV; EPRINTSEV, 2016; THALMANN et al., 2016).

Conclusions

The *Vitis* varieties BDMG573 and P1103 showed distinct metabolic responses when co-cultured with *Fusarium oxysporum* f.sp. *herbemontis*. At 4 DAT and 8 DAT, the BDMG573_CNT and BDMG573_FUS groups had a greater separation of areas denoting metabolic differences represented by a large number of differentially modulated metabolites. The sugar maltose was a common positive metabolite at both times of *Fusarium* co-culture that was indicated as a potential biomarker. Overall, there was an increase of glicolysis since sucrose and glucose were decreased and others monossacarides accumulated, as well as malate and citrate were drained from TCA to keep basic levels of aminoacids (Figure 10A).

In roots of the this genotype, there was more similarity between the metabolic profiles of the BDMG573_CNT and BDMG573_FUS at 0 DAT, and differences were accentuated at other days with the increasing number of significant metabolites. Both cellobiose and sorbitol were common at 4 DAT and 8 DAT demonstrating potential biomarkers. Thus, after 4 days of co-culture there is a change in primary metabolism enhancing the presence of carbohydrates from sucrose and glucose to stand with the infection process that is accentuated at 8 DAT, which leads to increase the number of significant amino acids related to signaling infection and as well as urea related to nitrogen metabolism as a source of nutrition (Figure 10B).

Conversely, in the P1103 genotype, 4 DAT and 8 DAT were similar in the shoots, and the 0 DAT and 4 DAT were similar in the roots. Since there are overlapping between the CNT and FUS groups in the response of *Fusarium* co-cultivation process over time. However, the maintainance of glicolisys, TCA and amino acids metabolism in the shoots co-cultivated with *Fusarium* was clear by the increase of primary metabolites in all times evaluated (Figure 8A). It may be related to the well-known better performance of this genotype upon biotic stress. In general, the OPLS-DA projected some organic acids at (0 DAT) amino acids (4 DAT) and carbohydrates (8 DAT) in the shoots, and mainly sugars in the roots (at all DAT's), configuring a metabolic adaptation of this genotype to abiotic and biotic stresses.

Figure 10 - Metabolic pathways modulated in shoots (a) and roots (b) of the two varieties of Vitis sp BDMG573 and P1103 co-cultivated with Fusarium oxysporum. The colors indicate the significant fold change of metabolites. Each square represents the log2 mean of four replicates. The color map shows an increasing (red scale) or decreasing (blue scale) of each metabolite in comparison to control plants.

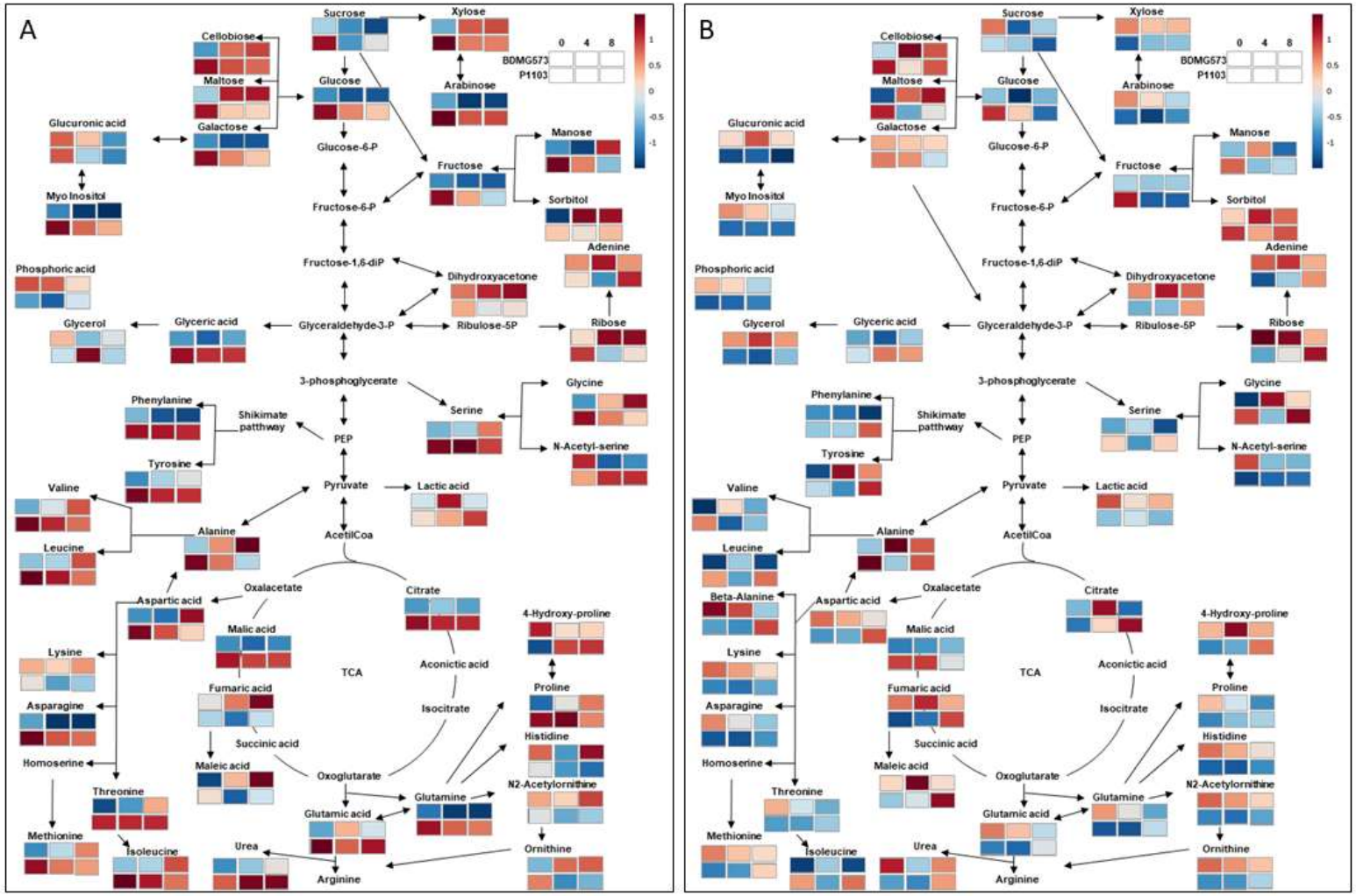

Supplementary material

Table S1. Loading scores of metabolites found shoots ranked by principal component analysis values.

Shoots at 0 DAT				Shoots at 4 DAT				Shoots at 8 DAT			
Metabolite	**PC1**	**Metabolite**	**PC2**	**Metabolite**	**PC1**	**Metabolite**	**PC2**	**Metabolite**	**PC1**	**Metabolite**	**PC2**
Aspartic acid	0.21686	Lysine	0.30382	Threonine	0.21514	Sucrose	0.28002	Aspartic acid	0.23497	Phosphoric acid	0.21223
Citric acid	0.21538	N2-Acet-Ornit	0.30016	Citric acid	0.21266	myo-Inositol	0.22986	Glycine	0.23369	Lysine	0.17841
Glutamine	0.21458	Adenine	0.28833	Glyceric acid	0.20853	Histidine	0.17608	Sorbitol	0.23259	N2-Acet-Ornit	0.15488
Glyceric acid	0.21126	1,3-Dihydroxyacet	0.28369	Malic acid	0.20639	Glutamine	0.17538	Maltose	0.22007	Ornithine	0.14264
Glucose	0.21018	Ribose	0.27957	Glucose	0.19291	Galactose	0.16322	Ribose	0.21653	1,3-dihydroxyacet	0.13158
Galactose	0.21018	Histidine	0.24885	Galactose	0.1929	Glucose	0.16317	Maleic acid	0.21537	Glycerol	0.11443
Tyrosine	0.20984	Phosphoric acid	0.24787	Glutamine	0.1903	Asparagine	0.16047	Fumaric acid	0.21268	Fumaric acid	0.10932
Glutamic acid	0.20969	Ornithine	0.23563	Leucine	0.18791	Arabinose	0.15448	Xylose	0.20964	Lactic acid	0.07323
Fructose	0.2062	Sucrose	0.20562	Isoleucine	0.18791	Fructose	0.12923	Cellobiose	0.20098	Alanine	0.057201
Malic acid	0.20072	Glycerol	0.18878	Fructose	0.18029	Lysine	0.10791	Alanine	0.18942	Histidine	0.047728
4-hydroxy-Prol	0.19112	Serine	0.18172	Tyrosine	0.17875	N2-Acet-Ornit	0.10502	Isoleucine	0.18265	Ribose	0.044157
Glycine	0.18247	Glucuronic acid	0.1787	Valine	0.17299	Malic acid	0.10027	Leucine	0.18265	Sorbitol	0.020351
Xylose	0.18017	Phenylalanine	0.17343	Arabinose	0.16943	N-acetyl-Ser	0.099704	1,3-Dihydroxyacet	0.1816	Sucrose	0.010036
Valine	0.17927	Arabinose	0.15028	Urea	0.16866	Glyceric acid	0.08873	Serine	0.18112	Glucuronic acid	0.001100
myo-Inositol	0.17553	myo-Inositol	0.14156	Phenylalanine	0.16721	Phenylalanine	0.087138	Threonine	0.17745	Maleic acid	-0.012406
Urea	0.17009	Asparagine	0.13817	Asparagine	0.16382	Mannose	0.077525	Valine	0.17348	Urea	-0.01733
Alanine	0.16831	Xylose	0.13744	4-hydroxy-Prol	0.15641	Phosphoric acid	0.023239	Adenine	0.16117	Glycine	-0.024916
Arabinose	0.16685	Fumaric acid	0.1318	Mannose	0.15526	Glucuronic acid	0.022678	Methionine	0.15704	Mannose	-0.026338
Threonine	0.16509	N-acetyl-Ser	0.12623	Aspartic acid	0.15444	Ornithine	0.020539	Proline	0.15442	Valine	-0.039584
Mannose	0.15912	Proline	0.086256	Glycine	0.14473	Maleic acid	0.015816	4-hydroxy-Prol	0.14407	Isoleucine	-0.043248
Asparagine	0.1589	Glutamic acid	0.075064	Methionine	0.14323	Aspartic acid	-0.004266	Mannose	0.12555	Leucine	-0.043248
Proline	0.15741	Mannose	0.044812	Glutamic acid	0.13154	Threonine	-0.0085098	Tyrosine	0.12197	Aspartic acid	-0.043621
Leucine	0.15423	Tyrosine	0.035137	Glycerol	0.11042	Fumaric acid	-0.011307	N2-Acet-Ornit	0.10418	Cellobiose	-0.047611
Isoleucine	0.15423	Fructose	0.020803	Proline	0.096429	Glycerol	-0.027306	Glutamic acid	0.10075	Maltose	-0.06043
Cellobiose	0.15214	Isoleucine	0.017457	Alanine	0.093866	Serine	-0.048222	Urea	0.074017	Adenine	-0.069363
Sucrose	0.13225	Leucine	0.017457	myo-Inositol	0.093517	Adenine	-0.061778	Histidine	0.071557	Xylose	-0.10776
Phenylalanine	0.1211	4-hydroxy-Prol	0.016903	N-acetyl-Ser	0.087893	Citric acid	-0.068445	Lysine	0.054041	Asparagine	-0.11561
Methionine	0.11495	Aspartic acid	0.0020189	Serine	0.079483	Methionine	-0.084708	Ornithine	0.027569	myo-Inositol	-0.1282
Serine	0.11288	Methionine	-0.0051155	Xylose	0.078816	Proline	-0.099448	Glycerol	0.017361	Serine	-0.13504
Maltose	0.10761	Maltose	-0.014298	Maltose	0.048726	Urea	-0.105	Lactic acid	-1.58E-04	Threonine	-0.13537
Maleic acid	0.057695	Galactose	-0.016158	Cellobiose	0.025613	Tyrosine	-0.11342	Glyceric acid	-0.014915	Fructose	-0.13693
Histidine	0.05341	Glucose	-0.016158	Lactic acid	-0.0027193	Isoleucine	-0.11959	Phosphoric acid	-0.01767	Methionine	-0.16553
Glucuronic acid	0.051614	Valine	-0.033459	Histidine	-0.02773	Leucine	-0.11959	Citric acid	-0.027543	Arabinose	-0.17456
Lactic acid	0.039405	Citric acid	-0.035876	Sucrose	-0.042277	Valine	-0.1533	Phenylalanine	-0.040633	Proline	-0.17479
Adenine	0.020126	Glutamine	-0.037672	Sorbitol	-0.086567	Glutamic acid	-0.16103	N-acetyl-Ser	-0.054644	4-hydroxy-Prol	-0.17824
1,3-dihydroxyace	-0.007559	Threonine	-0.037717	Glucuronic acid	-0.10227	Ribose	-0.17319	Galactose	-0.064216	Phenylalanine	-0.18745
N-acetyl-Ser	-0.013979	Glyceric acid	-0.043726	1,3-dihydroxyac	-0.12357	4-hydroxy-Prol	-0.1781	Glucose	-0.064216	Galactose	-0.21395
Fumaric acid	-0.03091	Alanine	-0.07258	Maleic acid	-0.126	1,3-dihydroxyace	-0.18426	Malic acid	-0.070654	Glucose	-0.21395
Lysine	-0.038176	Malic acid	-0.078595	Ribose	-0.13137	Xylose	-0.18508	Fructose	-0.07431	Glutamine	-0.2162
Ribose	-0.042896	Cellobiose	-0.079578	Adenine	-0.13245	Alanine	-0.19396	Glucuronic acid	-0.076735	Glutamic acid	-0.24247
N2-Acet-Ornit	-0.052718	Lactic acid	-0.089296	Lysine	-0.14312	Cellobiose	-0.20619	Arabinose	-0.13025	N-acetyl-Ser	-0.24494
Glycerol	-0.062742	Maleic acid	-0.10092	N2-Acet-Ornit	-0.14584	Glycine	-0.23172	Glutamine	-0.13716	Tyrosine	-0.25235
Sorbitol	-0.10163	Sorbitol	-0.11185	Fumaric acid	-0.18113	Maltose	-0.26428	Asparagine	-0.15653	Malic acid	-0.27491
Phosphoric acid	-0.1219	Glycine	-0.12504	Ornithine	-0.19918	Lactic acid	-0.27777	myo-Inositol	-0.18157	Glyceric acid	-0.27625
Ornithine	-0.12724	Urea	-0.14293	Phosphoric acid	-0.2015	Sorbitol	-0.28286	Sucrose	-0.2226	Citric acid	-0.28044

Table S2. Loading scores of metabolites found roots ranked by principal component analysis values.

Rhoots at 0 DAT				Rhoots at 4 DAT				Rhoots at 8 DAT			
Metabolite	**PC1**	**Metabolite**	**PC2**	**Metabolite**	**PC1**	**Metabolite**	**PC2**	**Metabolite**	**PC1**	**Metabolite**	**PC2**
Mannose	0.17949	Glycine	0.30915	Malic acid	0.14851	Sucrose	0.27789	Sorbitol	0.22178	Adenine	0.24872
Malic acid	0.15244	Serine	0.2866	Sorbitol	0.059204	Phenylalanine	0.24153	Ribose	0.21172	Methionine	0.24716
Cellobiose	0.13476	Leucine	0.27403	Mannose	0.02837	Glucose	0.2286	Urea	0.20614	Fumaric acid	0.23977
Glucose	0.10193	Isoleucine	0.27403	Glyceric acid	0.0013586	N-acetyl-Serine	0.17492	Cellobiose	0.20294	Aspartic acid	0.23465
Sorbitol	0.098548	Alanine	0.27398	Glucose	-0.0012919	Glyceric acid	0.17424	Glycine	0.18201	1,3-Dihydroxyacet	0.23349
Fructose	0.08741	Valine	0.25371	Citric acid	-0.010579	Glutamine	0.13349	Alanine	0.16941	B-alanine	0.22504
Glycine	0.028884	Phenylalanine	0.25285	Urea	-0.019456	Serine	0.13188	Maleic acid	0.14578	4-hydroxy-Proline	0.21267
Maltose	0.028765	Fructose	0.25052	Cellobiose	-0.027609	Isoleucine	0.13003	Tyrosine	0.13497	Ornithine	0.2126
Alanine	0.023333	Glucose	0.22529	Sucrose	-0.051034	Leucine	0.13003	Glyceric acid	0.11541	Glutamic acid	0.19042
Tyrosine	0.019613	Glyceric acid	0.22457	Maleic acid	-0.068976	Fructose	0.12303	Fumaric acid	0.10609	Xylose	0.18164
Valine	-0.0082589	Ribose	0.21502	Alanine	-0.0766	Asparagine	0.11676	1,3-Dihydroxyacet	0.081843	Maleic acid	0.17631
Leucine	-0.012752	Citric acid	0.17746	Galactose	-0.083052	Threonine	0.10931	4-hydroxy-Proline	0.068132	N2-Acetyl-Ornit	0.15816
Isoleucine	-0.012752	Malic acid	0.16982	Ribose	-0.084586	Arabinose	0.096921	Maltose	0.057389	Lysine	0.15651
Glucuronic acid	-0.029418	Cellobiose	0.15844	Fructose	-0.084998	Proline	0.083887	Citric acid	0.043835	Alanine	0.12919
Citric acid	-0.030008	Maltose	0.13687	N-acetyl-Serine	-0.09141	Phosphoric acid	0.080667	Adenine	0.020787	Tyrosine	0.11981
Ribose	-0.060345	Lactic acid	0.12619	Tyrosine	-0.098569	Urea	0.076713	Aspartic acid	0.016013	Glycine	0.1197
Galactose	-0.068104	Sorbitol	0.11562	Phenylalanine	-0.1068	Malic acid	0.068112	B-alanine	0.015666	Cellobiose	0.11627
N-acetyl-Serine	-0.073872	Mannose	0.11433	Lactic acid	-0.12933	Valine	0.066298	Mannose	0.0030865	Histidine	0.11101
Lactic acid	-0.077264	Sucrose	0.11419	1,3-Dihydroxyacet	-0.14121	myo-Inositol	0.053664	Lactic acid	-0.032157	Glycerol	0.10759
Serine	-0.077293	N-acetyl-Serine	0.10436	Adenine	-0.14223	Lactic acid	0.044057	Malic acid	-0.056256	Threonine	0.1055
Glyceric acid	-0.091369	4-hydroxy-Proline	0.10161	Glycine	-0.14283	Glutamic acid	0.027633	Phenylalanine	-0.057524	Lactic acid	0.10481
Phenylalanine	-0.094471	Threonine	0.097643	4-hydroxy-Proline	-0.15194	Histidine	0.018333	Glycerol	-0.061672	Ribose	0.10077
Urea	-0.099258	Urea	0.093874	Isoleucine	-0.15299	Methionine	0.0046442	Galactose	-0.062072	Isoleucine	0.099337
B-alanine	-0.1321	Glutamine	0.081372	Leucine	-0.15299	Xylose	0.0019583	Isoleucine	-0.069783	Leucine	0.099337
Sucrose	-0.14175	Phosphoric acid	0.069586	Asparagine	-0.15973	Lysine	-0.004651	Leucine	-0.069783	Maltose	0.099072
Maleic acid	-0.17056	Galactose	0.04635	Glucuronic acid	-0.16114	N2-Acetyl-Ornit	-0.015095	Methionine	-0.070379	Galactose	0.09814
Adenine	-0.17697	Proline	0.046216	Glutamine	-0.16708	Aspartic acid	-0.028508	Proline	-0.11932	Citric acid	0.093133
Glutamine	-0.17917	Asparagine	0.032716	Valine	-0.16786	Maltose	-0.030793	Xylose	-0.12095	Valine	0.092293
Fumaric acid	-0.1851	1,3-Dihydroxyacet	0.031588	Glycerol	-0.16881	Ornithine	-0.040862	Ornithine	-0.1258	Glutamine	0.085139
1,3-Dihydroxyaceton	-0.18631	Glutamic acid	0.030664	Serine	-0.17343	Glucuronic acid	-0.060648	Serine	-0.12953	Proline	0.076741
Phosphoric acid	-0.19003	Aspartic acid	0.0075728	Proline	-0.17452	Mannose	-0.060845	Valine	-0.1537	Serine	0.067594
4-hydroxy-Prol	-0.19085	Xylose	0.0046845	Arabinose	-0.17541	Glycerol	-0.063944	Glucuronic acid	-0.15438	Sorbitol	0.058573
Proline	-0.19623	myo-Inositol	-0.013536	Xylose	-0.17841	Galactose	-0.090588	Fructose	-0.15567	Arabinose	0.05537
Asparagine	-0.19705	Methionine	-0.017485	Fumaric acid	-0.17898	B-alanine	-0.10749	Glutamic acid	-0.15679	Phosphoric acid	0.048744
Histidine	-0.19707	Lysine	-0.019221	B-alanine	-0.1858	Fumaric acid	-0.12772	N2-Acetyl-Ornit	-0.17721	myo-Inositol	0.046579
Threonine	-0.19716	Glycerol	-0.019784	Glutamic acid	-0.18696	Glycine	-0.15425	Glutamine	-0.17852	Phenylalanine	0.038238
Arabinose	-0.19795	N2-Acetyl-Ornit	-0.029741	Threonine	-0.1882	Adenine	-0.15886	Lysine	-0.18262	Asparagine	0.018273
Aspartic acid	-0.19836	B-alanine	-0.036838	Maltose	-0.19494	Citric acid	-0.16445	Glucose	-0.18785	Urea	-0.08914
Glycerol	-0.19901	Ornithine	-0.037842	Phosphoric acid	-0.19571	Tyrosine	-0.18575	N-acetyl-Serine	-0.19177	Glucuronic acid	-0.09734
Glutamic acid	-0.20134	Arabinose	-0.045902	Aspartic acid	-0.19715	1,3-Dihydroxyac	-0.19909	Histidine	-0.20374	Sucrose	-0.1079
Xylose	-0.2025	Maleic acid	-0.050046	Methionine	-0.19823	4-hydroxy-Prol	-0.20065	Threonine	-0.20702	N-acetyl-Serine	-0.1091
Methionine	-0.20293	Adenine	-0.053198	myo-Inositol	-0.20135	Ribose	-0.25302	Sucrose	-0.21105	Glucose	-0.15619
Ornithine	-0.2065	Glucuronic acid	-0.080319	Histidine	-0.20191	Maleic acid	-0.25584	Asparagine	-0.21489	Glyceric acid	-0.17295
myo-Inositol	-0.20855	Histidine	-0.08342	Ornithine	-0.2043	Alanine	-0.25805	Arabinose	-0.21722	Fructose	-0.18326
N2-Acetyl-Ornit	-0.20881	Fumaric acid	-0.085824	N2-Acetyl-Ornit	-0.20851	Sorbitol	-0.27349	Phosphoric acid	-0.22346	Malic acid	-0.20406
Lysine	-0.20947	Tyrosine	-0.086293	Lysine	-0.20993	Cellobiose	-0.29176	myo-Inositol	-0.2246	Mannose	-0.21583

Figure S1 – Variable importance in projection (VIP) scores of metabolites in shoots of Vitis genotypes BDMG573 (A, B, and C) and P1103 (D, E, and F) co-cultured with *Fusarium oxysporum* fungus (FUS) compared to non-co-cultivated (CNT).

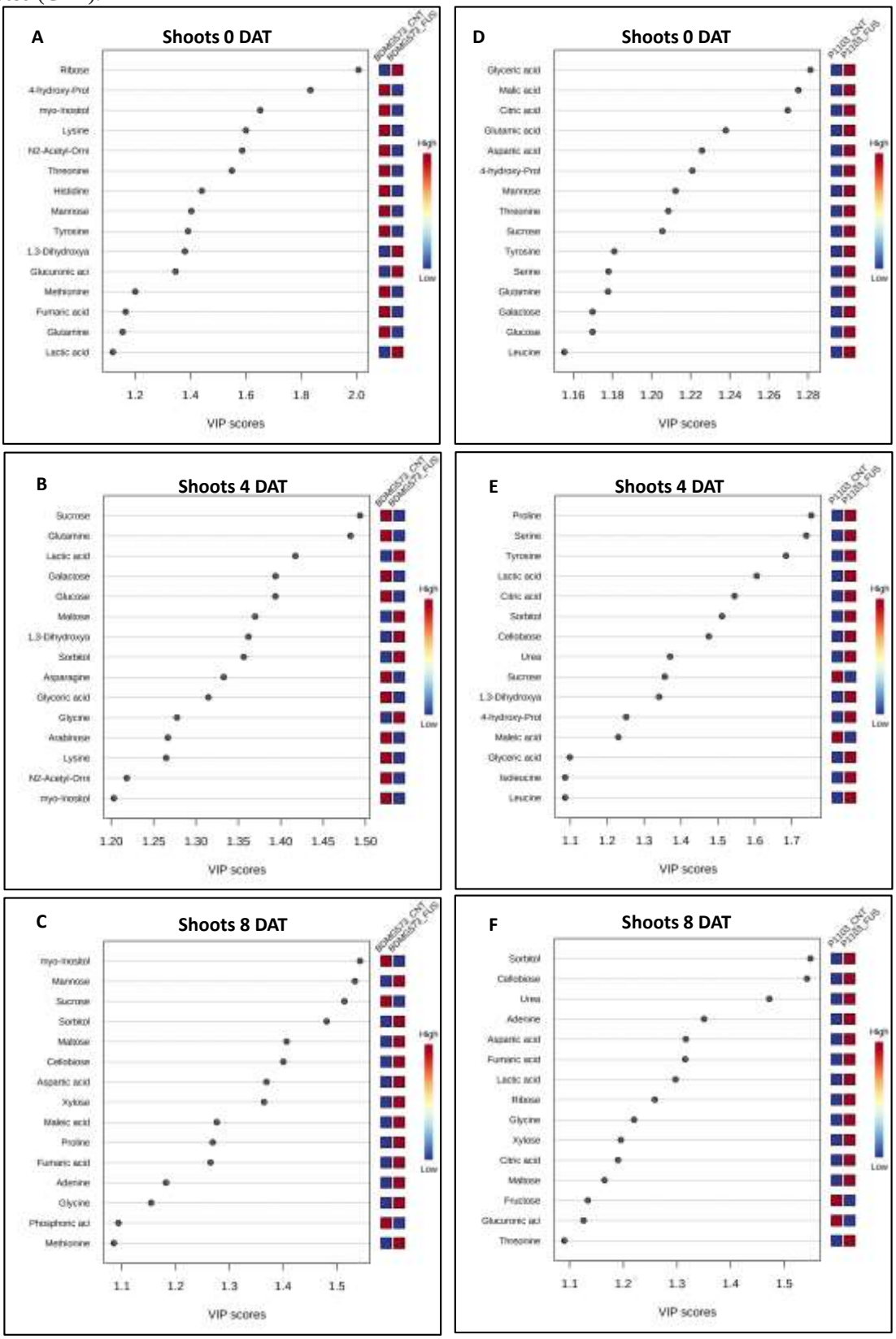

Figure S2 – Variable importance in projection (VIP) scores of metabolites in rhoots of Vitis genotypes BDMG573 (A, B, and C) and P1103 (D, E, and F) co-cultured with *Fusarium oxysporum* fungus (FUS) compared to non-co-cultivated (CNT).

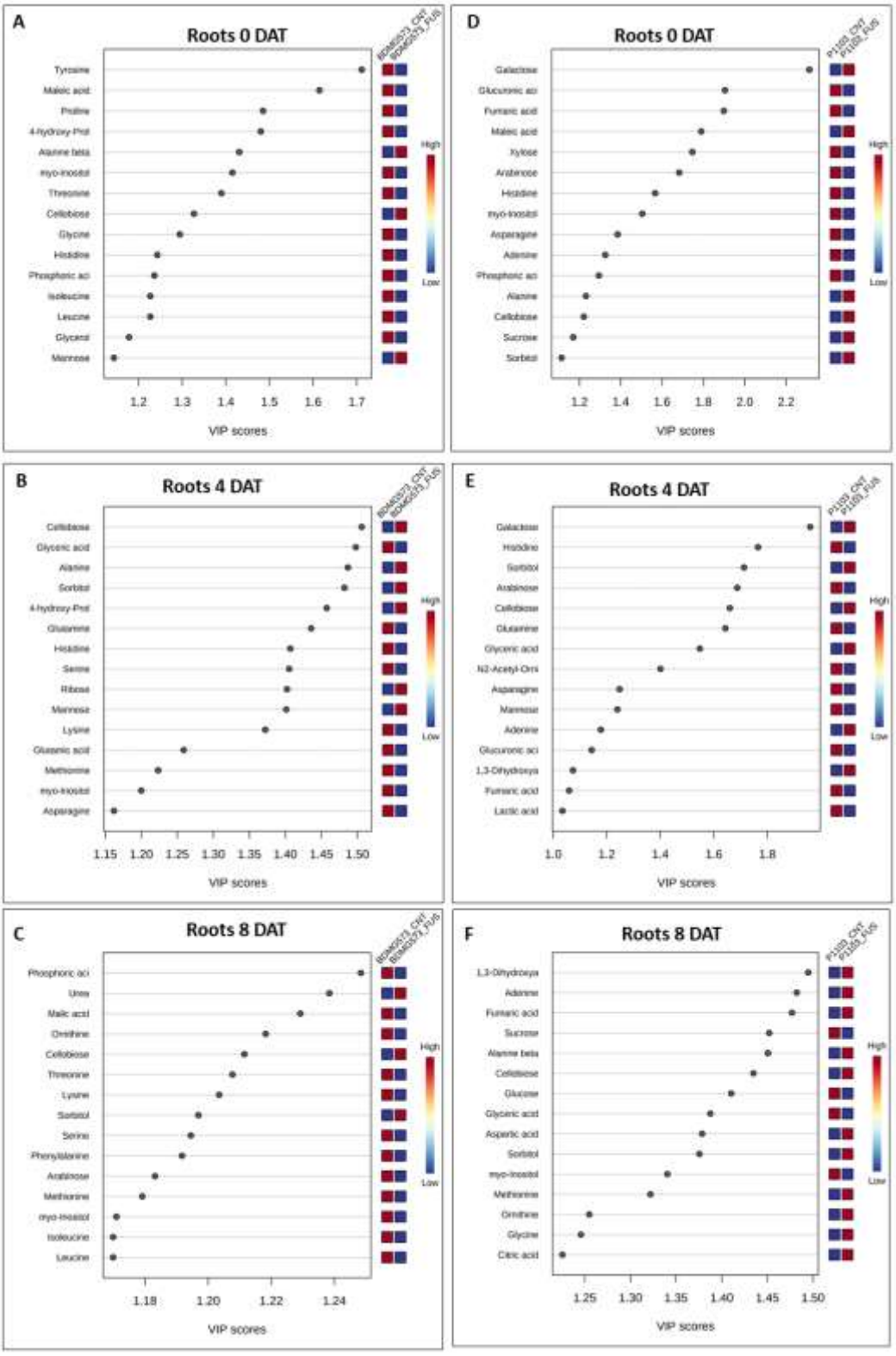

5. CONSIDERAÇÕES FINAIS

No geral, este trabalho proporciona um progresso significativo na resposta ao estresse do *Fusarium oxysporum* explorando metabólitos diferencialmente modulados e potenciais marcadores para dois genótipos de Vitis. Embora os dados sejam reunidos numa via metabolica apresentando glicólise, ciclo dos ácidos tricarboxilicos e metabolismo de vários aminoácidos, a relação entre açúcares e outros metabólitos para fornecer energia e síntese de outras moléculas de defesa ainda precisa ser mais explorada no futuro. Além disso, a maior incidência de açúcares nas raizes do que em relação as shoots de ambos os genótipos co-cultivados com *Fusarium* podem ter o potencial de ajudar as plântulas a sobreviver, como observado para o genótipo P1103 onde foi notado uma maior variedade de açúcares e uma modulação mais positiva do grupo co-cultivado em relação ao controle, especialmente pela manutenção dos componentes da glicólise e ciclo dos ácidos tricarboxílicos.

REFERÊNCIAS

ALSEEKH, S. et al. Mass spectrometry-based metabolomics: a guide for annotation, quantification and best reporting practices. **Nature Methods**, v. 18, n. 7, p. 747–756, 2021.

ANDRADE, E. R. et al. Evaluation of grapevine (Vitis spp.) resistance to Fusarium oxysporum f. sp. herbemontis in Rio de peixe valley, Santa Catarina State, Brazil. **Acta Horticulture Viticunture and Enolology**, v. 388, p. 65–69, 1995.

ARIE, T. et al. Immunological Detection of endoPolygalacturonase Secretion by Fusarium oxysporum in Plant Tissue and Sequencing of Its Encoding Gene. **Japanese Journal of Phytopathology**, v. 64, n. 1, p. 7–15, 1998.

ARIE, T. **Fusarium diseases of cultivated plants, control, diagnosis, and molecular and genetic studies**. [s.l: s.n.]. v. 44

BAI, G.; SHANER, G. Management and resistance in wheat and barley to fusarium head blight. **Annual Review of Phytopathology**, v. 42, p. 135–161, 2004.

BAIDOO, E. E. K. Microbial metabolomics: A general overview. In: **Methods in Molecular Biology**. [s.l: s.n.]. v. 1859p. 1–8.

BEALE, D. J. et al. **Review of recent developments in GC–MS approaches to metabolomics-based research**. [s.l.] Springer US, 2018. v. 14

BEIER, M. P.; KOJIMA, S. The function of high-affinity urea transporters in nitrogen-deficient conditions. **Physiologia Plantarum**, v. 171, n. 4, p. 802–808, abr. 2021.

BERNARDO, S. et al. Grapevine abiotic stress assessment and search for sustainable adaptation strategies in Mediterranean-like climates. A review. **Agronomy for Sustainable Development**, v. 38, n. 6, 2018.

BERTSCH, C. et al. Grapevine trunk diseases: Complex and still poorly understood. **Plant Pathology**, v. 62, n. 2, p. 243–265, 2013.

BIGEARD, J.; COLCOMBET, J.; HIRT, H. Signaling mechanisms in pattern-triggered immunity (PTI). **Molecular Plant**, v. 8, n. 4, p. 521–539, 2015.

BOUIZGARNE, B. et al. Early physiological responses of Arabidopsis thaliana cells to fusaric acid: Toxic and signalling effects. **New Phytologist**, v. 169, n. 1, p. 209–218, 2006.

BRUM, M. C. et al. Endophytic fungi from Vitis labrusca L. ('Niagara Rosada') and its potential for the biological control of Fusarium oxysporum. **Genetics and molecular research : GMR**, v. 11, n. 4, p. 4187–4197, 2012.

BUHTZ, A. et al. Perturbations in the primary metabolism of tomato and arabidopsis thaliana plants infected with the soil-borne fungus verticillium Dahliae. **PLoS ONE**, v. 10, n. 9, p. 1–14, 2015.

CANUTO, G. et al. Metabolômica: definições, estado-da-arte e aplicações representativas. **Química Nova**, v. 41, n. 1, p. 75–91, 2017.

CASTELLARIN, S. D. et al. Transcriptional regulation of anthocyanin biosynthesis in ripening fruits of grapevine under seasonal water deficit. **Plant, Cell and Environment**, v. 30, n. 11, p. 1381–1399, 2007.

CAVALCANTI, F. R. Co-cultivo in vitro pode discriminar severidade de podridões do tronco em genótipos de videira. **Comitê Local de Publicações da Embrapa Uva e Vinho -BOLETIM DE PESQUISA E DESENVOLVIMENTO 20**, n. 1981–1001, p. 2–38, 2021.

CHEN, F.; MA, R.; CHEN, X.-L. Advances of Metabolomics in Fungal Pathogen–Plant Interactions. **Metabolites**, v. 9, n. 8, p. 169, 15 ago. 2019.

CHEN, L. et al. Combined De Novo Transcriptome and Metabolome Analysis of Common Bean Response to Fusarium oxysporum f. sp. phaseoli Infection. **International Journal of Molecular Sciences**, v. 20, n. 24, p. 6278, 12 dez. 2019.

CHUBERRE, C. et al. Plant Immunity Is Compartmentalized and Specialized in Roots. **Frontiers in Plant Science**, v. 9, n. November, p. 1–13, 28 nov. 2018.

COLEMAN, A. D. et al. The Arabidopsis leucine-rich repeat receptor kinase MIK2 is a crucial component of pattern-triggered immunity responses to Fusarium fungi. **bioRxiv**, v. 11, n. 1, p. 1–14, 2019.

COSTA, M. D.; LOVATO, P. E.; SETE, P. B. Micorrização e indução de quitinases e β-1,3-glucanases e resistência à fusariose em porta-enxerto de videira. **Pesquisa Agropecuaria Brasileira**, v. 45, n. 4, p. 376–383, 2010.

CRAMER, G. R. Abiotic stress and plant responses from the whole vine to the genes. **Australian Journal of Grape and Wine Research**, v. 16, n. SUPPL. 1, p. 86–93, 2010.

DALDOUL, S. et al. Recent advances in biotechnological studies on wild grapevines as valuable resistance sources for smart viticulture. **Molecular Biology Reports**, v. 47, n. 4, p. 3141–3153, 2020.

DANIEL, R. M. et al. The molecular basis of the effect of temperature on enzyme activity. **Biochemical Journal**, v. 425, n. 2, p. 353–360, 2010.

DARKO, E. et al. Metabolic responses of wheat seedlings to osmotic stress induced by various osmolytes under iso-osmotic conditions. **PLoS ONE**, v. 14, n. 12, p. 1–19, 2019.

DE LAMO, F. J.; TAKKEN, F. L. W. Biocontrol by Fusarium oxysporum Using Endophyte-Mediated Resistance. **Frontiers in Plant Science**, v. 11, n. February, p. 1–15, 2020.

DESJARDINS., A. E. Fusarium Mycotoxins: Chemistry, Genetics and Biology - by Anne E. Desjardins. In: **Plant Pathology**. [s.l: s.n.]. v. 56p. 337–337.

DING, Z. et al. Fusaric acid is a virulence factor of Fusarium oxysporum f. sp. cubense on banana plantlets. **Tropical Plant Pathology**, v. 43, n. 4, p. 297–305, 2018.

DURRANT, W. E.; DONG, X. SYSTEMIC ACQUIRED RESISTANCE. **Annual Review of Phytopathology**, v. 42, n. 1, p. 185–209, 1 set. 2004.

DWEBA, C. C. et al. Fusarium head blight of wheat: Pathogenesis and control strategies. **Crop Protection**, v. 91, p. 114–122, 2017.

EDWARDS, J. et al. Relationships between grape phylloxera abundance, fungal interactions and grapevine decline. **Acta Horticulturae**, v. 733, p. 151–157, 2007.

EVELAND, A. L.; JACKSON, D. P. Sugars, signalling, and plant development. **Journal of Experimental Botany**, v. 63, n. 9, p. 3367–3377, 2012.

FEUSSNER, I.; POLLE, A. What the transcriptome does not tell - proteomics and metabolomics are closer to the plants' patho-phenotype. **Current Opinion in Plant Biology**, v. 26, p. 26–31, 2015.

FIEHN, O. Metabolomics - The link between genotypes and phenotypes. **Plant Molecular Biology**, v. 48, n. 1–2, p. 155–171, 2002.

FIEHN, O. Extending the breadth of metabolite profiling by gas chromatography coupled to mass spectrometry. **TrAC - Trends in Analytical Chemistry**, v. 27, n. 3, p. 261–269, 2008.

FRAGA, H. et al. Climatic suitability of Portuguese grapevine varieties and climate change adaptation. **International Journal of Climatology**, v. 36, n. 1, p. 1–12, 2016.

GARRIDO, L. DA R.; SÔNEGO, O. R. Chave para identificação de agentes causadores de declínio da videira. Circular Técnica 26. **Comitê Local de Publicações da Embrapa Uva e Vinho**, p. 1–20, 1999.

GARRIDO, L. DA R.; SÔNEGO, O. R.; GOMES, V. N. Chave para identificação de agentes causadores de declínio da videeira -. **Fitopatologia Brasileira**, v. 29, n. 3, p. 322–324, 2004a.

GARRIDO, L. DA R.; SÔNEGO, O. R.; GOMES, V. N. Fungos associados com o declínio e morte de videiras no estado do Rio Grande do Sul. **Fitopatologia Brasileira**, v. 29, n. 3, p. 322–324, jun. 2004b.

GONÇALVES, A. Z. et al. Thinking of the leaf as a whole plant: How does N metabolism occur in a plant with foliar nutrient uptake? **Environmental and Experimental Botany**, v. 178, 2020.

GORDON, T. R. Fusarium oxysporum and the Fusarium Wilt Syndrome. **Annual Review of Phytopathology**, v. 55, p. 23–39, 2017.

GRAMAJE, D.; URBEZ-TORRES, J. R.; SOSNOWSKI, M. R. Managing grapevine trunk diseases with respect to etiology and epidemiology: Current strategies and future prospects. **Plant Disease**, v. 102, n. 1, p. 12–39, 2018.

GRANATO, D. et al. Use of principal component analysis (PCA) and hierarchical cluster analysis (HCA) for multivariate association between bioactive compounds and functional properties in foods: A critical perspective. **Trends in Food Science and Technology**, v. 72, n. 2018, p. 83–90, 2018.

GUPTA, S. et al. Primary Metabolism of Chickpea Is the Initial Target of Wound Inducing Early Sensed Fusarium oxysporum f. sp. ciceri Race I. **PLoS ONE**, v. 5, n. 2, p. e9030, 3 fev. 2010.

HACQUARD, S. et al. Annual Review of Phytopathology Interplay Between Innate Immunity and the Plant Microbiota. **The Annual Review ofPhytopathology**, 2017.

HENRY, G.; THONART, P.; ONGENA, M. PAMPs, MAMPs, DAMPs and others: an update on the diversity of plant immunity elicitors. **Biotechnol. Agron. Soc. Environ**, v. 16, p. 257–268, 2012.

HEUBERGER, A. L. et al. Evaluating plant immunity using mass spectrometry-based metabolomics workflows. **Frontiers in Plant Science**, v. 5, n. JUN, p. 1–12, 2014.

HOECKEL, P. H. D. O.; FREITAS, C. A. DE; FEISTEL, P. R. A política comercial brasileira e sua influência no setor vitivinícola. **Perspectiva Econômica**, v. 13, n. 1, p. 24–43, 2017.

HUMBERT, C. et al. Remodelling of actin cytoskeleton in tomato cells in response to inoculation with a biocontrol strain of Fusarium oxysporum in comparison to a pathogenic strain. **Plant Pathology**, v. 64, n. 6, p. 1366–1374, 2015.

IGAMBERDIEV, A. U.; EPRINTSEV, A. T. Organic Acids: The Pools of Fixed Carbon Involved in Redox Regulation and Energy Balance in Higher Plants. **Frontiers in Plant Science**, v. 7, n. 2016JULY, p. 1–15, 15 jul. 2016.

JUNGES, A. H.; SANTOS, H. P. DOS; GARRIDO, L. DA R. Condições meteorológicas de outubro a dezembro de 2020 , prognóstico climático para janeiro-fevereiro-março de 2021 e recomendações fitotécnicas para vinhedos. **Boletin Agrometeorólogico da Serra Gaúcha - Embrapa Uva e Vinho**, n. 1, p. 21, 2022.

KASOTE, D. M. et al. Metabolomics-based biomarkers of Fusarium wilt disease in watermelon plants. **Journal of Plant Diseases and Protection**, v. 127, n. 4, p. 591–596, 21 ago. 2020.

KELL, D. B. et al. Metabolic footprinting and systems biology: The medium is the message. **Nature Reviews Microbiology**, v. 3, n. 7, p. 557–565, 2005.

KHAKIMOV, B.; JESPERSEN, B. M.; ENGELSEN, S. B. Comprehensive and comparative metabolomic profiling of wheat, barley, oat and rye using gas chromatography-mass spectrometry and advanced chemometrics. **Foods**, v. 3, n. 4, p. 569–585, 2014.

KHAN, M. M. et al. Role of grapevine rootstocks in mitigating environmental stresses: A review. **Journal of Agricultural and Marine Sciences [JAMS]**, v. 25, n. 2, p. 1, 2020.

KIDD, B. N. et al. Auxin Signaling and Transport Promote Susceptibility to the Root-Infecting Fungal Pathogen Fusarium oxysporum in Arabidopsis. **Molecular Plant-Microbe Interactions®**, v. 24, n. 6, p. 733–748, jun. 2011.

KOCZYK, G.; DAWIDZIUK, A.; POPIEL, D. The distant siblings - A phylogenomic roadmap illuminates the origins of extant diversity in fungal aromatic polyketide biosynthesis. **Genome Biology and Evolution**, v. 7, n. 11, p. 3132–3154, 2015.

KRUMPOCHOVA, P. et al. Amino acid analysis using chromatography-mass spectrometry: An inter platform comparison study. **Journal of Pharmaceutical and Biomedical Analysis**, v. 114, p. 398–407, 2015.

KUEHNBAUM, N. L.; BRITZ-MCKIBBIN, P. New advances in separation science for metabolomics resolving. **Chemical Reviews**, v. 113, n. 4, p. 2437–2468, 2013.

KUMAR, Y. et al. Metabolic profiling of chickpea-Fusarium interaction identifies differential modulation of disease resistance pathways. **Phytochemistry**, v. 116, n. 1, p. 120–129, 2015.

LAGOPODI, A. L. et al. Novel Aspects of Tomato Root Colonization and Infection by Fusarium oxysporum f. sp. radicis-lycopersici Revealed by Confocal Laser Scanning Microscopic Analysis Using the Green Fluorescent Protein as a Marker. **Molecular Plant-Microbe Interactions®**, v. 15, n. 2, p. 172–179, fev. 2002.

LANUBILE, A. et al. Transcriptome profiling of soybean (Glycine max) roots challenged with pathogenic and non-pathogenic isolates of Fusarium oxysporum. **BMC Genomics**, v. 16, n. 1, p. 1–14, 2015.

LASTDRAGER, J.; HANSON, J.; SMEEKENS, S. Sugar signals and the control of plant growth and development. **Journal of Experimental Botany**, v. 65, n. 3, p. 799–807, 2014.

LECOMTE, P. et al. New insights into Esca of grapevine: The development of foliar symptoms and their association with xylem discoloration. **Plant Disease**, v. 96, n. 7, p. 924–934, 2012.

LEI, H. et al. Fermentation performance of lager yeast in high gravity beer fermentations with different sugar supplementations. **Journal of Bioscience and Bioengineering**, v. 122, n. 5, p. 583–588, 2016.

LI, Z. et al. Metabolomics and physiological analyses reveal β-sitosterol as an important plant growth regulator inducing tolerance to water stress in white clover. **Planta**, v. 250, n. 6, p. 2033–2046, 2019.

LISEC, J. et al. Gas chromatography mass spectrometry-based metabolite profiling in plants. **Nature Protocols**, v. 1, n. 1, p. 387–396, 2006.

MACHO, A. P.; ZIPFEL, C. Plant PRRs and the activation of innate immune signaling. **Molecular Cell**, v. 54, n. 2, p. 263–272, 2014.

MELLO, L. M. R. DE; MACHADO, C. A. E. Vitivinicultura brasileira : Panorama 2019. Comunicado Técnico 214. Embrapa. **Comitê Local de Publicações da Embrapa Uva e Vinho**, n. 1808–6802, p. 1–21, 2020.

MENG, D. et al. Sorbitol Modulates Resistance to Alternaria alternata by Regulating the Expression of an NLR Resistance Gene in Apple. **The Plant Cell**, v. 30, n. 7, p. 1562–1581, jul. 2018.

MEVIK, B.-H.; WEHRENS, R. The pls Package: Principal Component and Partial Least Squares Regression in R. **Journal of Statistical Software**, v. 18, n. 2, p. 1–24, 2007.

MONDELLO, V. et al. Grapevine Trunk Diseases: A Review of Fifteen Years of Trials for Their Control with Chemicals and Biocontrol Agents. **Plant Disease**, v. 102, n. 7, p. 1189–1217, jul. 2018.

MORSCH, L. et al. Root system structure as a criterion for the selection of grapevine genotypes that are tolerant to excess copper and the ability of P to mitigate toxicity. **Plant Physiology and Biochemistry**, v. 171, n. December 2021, p. 147–156, 2021.

MUGNAI, L.; GRANITI, A.; SURICO, G. Esca (Black measles) and brown wood-streaking: Two old and elusive diseases of grapevines. **Plant Disease**, v. 83, n. 5, p. 404–418, 1999.

MUNDY, D. C.; MANNING, M. A. Ecology and management of grapevine trunk diseases in New Zealand: A review. **New Zealand Plant Protection**, v. 63, p. 160–166, 2010.

MUR, L. A. J. et al. The hypersensitive response; The centenary is upon us but how much do we know? **Journal of Experimental Botany**, v. 59, n. 3, p. 501–520, 2008.

MURASHIGE, T.; SKOOG, F. Murashige1962Revised.Pdf. **Physiologia Plantarum**, v. 15, p. 474–497, 1962.

NAKABAYASHI, R.; SAITO, K. Integrated metabolomics for abiotic stress responses in plants. **Current Opinion in Plant Biology**, v. 24, p. 10–16, abr. 2015.

O'BRIEN, J. A. et al. Reactive oxygen species and their role in plant defence and cell wall metabolism. **Planta**, v. 236, n. 3, p. 765–779, 2012.

OLIVERI, P.; SIMONETTI, R. **Chemometrics for Food Authenticity Applications**. [s.l.] Elsevier Ltd, 2016.

OLLAT, N. et al. Rootstocks as a component of adaptation to environment. In: HERNÂNI GERÓS, MARIA MANUELA CHAVES, H. M. G. AND S. D. (Ed.). . **Grapevine in a Changing Environment: A Molecular and Ecophysiological Perspective**. [s.l.] John Wiley & Sons, Ltd., 2016. p. 68–108.

PAPADOPOULOU, G. V. et al. Defence signalling marker gene responses to hormonal elicitation differ between roots and shoots. **AoB PLANTS**, v. 10, n. 3, p. 1–15, 2018.

PARTHASARATHY, A.; SAVKA, M. A.; HUDSON, A. O. The Synthesis and Role of β-Alanine in Plants. **Frontiers in Plant Science**, v. 10, n. July, 18 jul. 2019.

PAVLOUSEK, P. Evaluation of drought tolerance of new grapevine rootstock hybrids. **Journal of Environmental Biology**, v. 32, n. 5, p. 543–549, 2011.

PEDERSEN, B. H. Determination of graft compatibility in sweet cherry by a co-culture method. **Journal of Horticultural Science and Biotechnology**, v. 81, n. 4, p. 759–764, 2006.

PILON, A. et al. Metabolômica De Plantas: Métodos E Desafios. **Química Nova**, v. 43, n. 3, p. 329–354, 2020.

PROCTOR, R. H. et al. Co-expression of 15 contiguous genes delineates a fumonisin biosynthetic gene cluster in Gibberella moniliformis. **Fungal Genetics and Biology**, v. 38, n. 2, p. 237–249, 2003.

PROCTOR, R. H. et al. Birth, death and horizontal transfer of the fumonisin biosynthetic gene cluster during the evolutionary diversification of fusarium. **Molecular Microbiology**, v. 90, n. 2, p. 290–306, 2013.

REINHART, V. **No Multiplicação de matrizes de porta-enxertos híbridos de videira (Vitis labrusca x Vitis rotundifolia) por micropropagação**. [s.l.] Universidade Federal do Paraná, 2013.

REVEGLIA, P. et al. The main phytotoxic metabolite produced by a strain of Fusarium oxysporum inducing grapevine plant declining in Italy. **Natural Product Research**, v. 32, n. 20, p. 2398–2407, 2018.

ROLLAND, F.; MOORE, B.; SHEEN, J. Sugar Sensing and Signaling in Plants. **The Plant Cell**, v. 14, n. suppl 1, p. S185–S205, 26 maio 2002.

ROLSHAUSEN, P. E. et al. Evaluation of pruning wound susceptibility and protection against fungi associated with grapevine trunk diseases. **American Journal of Enology and Viticulture**, v. 61, n. 1, p. 113–119, 2010.

RONCERO, M. I. G. et al. Fusarium as a model for studying virulence in soilborne plant pathogens. **Physiological and Molecular Plant Pathology**, v. 62, n. 2, p. 87–98, 2003.

SANKARAN, S. et al. A review of advanced techniques for detecting plant diseases. **Computers and Electronics in Agriculture**, v. 72, n. 1, p. 1–13, jun. 2010.

SEBASTIANI, M. S. et al. Transcriptome Analysis of the Melon-Fusarium oxysporum f. sp. melonis Race 1.2 Pathosystem in Susceptible and Resistant Plants. **Frontiers in Plant Science**, v. 8, n. March, p. 1–15, 17 mar. 2017.

SIDDAPPA, S.; MARATHE, G. K. What we know about plant arginases? **Plant Physiology and Biochemistry**, v. 156, n. June, p. 600–610, 2020.

SILVAA, P. M. DOS S. et al. Insights into anti-pathogenic activities of mannose lectins. **International Journal of Biological Macromolecules**, v. 140, p. 234–244, nov. 2019.

STĘPIEŃ, Ł. The use of Fusarium secondary metabolite biosynthetic genes in chemotypic and phylogenetic studies. **Critical Reviews in Microbiology**, v. 40, n. 2, p. 176–185, 2014.

SUN, X. et al. Roles of malic enzymes in plant development and stress responses. **Plant Signaling and Behavior**, v. 14, n. 10, p. 1–8, 2019.

SUSCA, A.; MORETTI, A.; LOGRIECO, A. F. Mycotoxin Biosynthetic Pathways: A Window on the Evolutionary Relationships Among Toxigenic Fungi Antonia. In: **Modern Tools and Techniques to Understand Microbes**. Bari, Italy: Springer International Publishing AG, 2017. p. 1–461.

TAN, K.-C. et al. Assessing the impact of transcriptomics, proteomics and metabolomics on fungal phytopathology. **Molecular Plant Pathology**, v. 10, n. 5, p. 703–715, set. 2009.

TEIXEIRA, A. et al. The first insight into the metabolite profiling of grapes from three Vitis vinifera L. cultivars of two controlled appellation (DOC) regions. **International Journal of Molecular Sciences**, v. 15, n. 3, p. 4237–4254, 2014.

THALMANN, M. et al. Regulation of leaf starch degradation by abscisic acid is important for osmotic stress tolerance in plants. **Plant Cell**, v. 28, n. 8, p. 1860–1878, 2016.

THÉVENOT, E. A. et al. Analysis of the Human Adult Urinary Metabolome Variations with Age, Body Mass Index, and Gender by Implementing a Comprehensive Workflow for Univariate and OPLS Statistical Analyses. **Journal of Proteome Research**, v. 14, n. 8, p. 3322–3335, 2015.

TUGIZIMANA, F. et al. Metabolomics in Plant Priming Research: The Way Forward? **International Journal of Molecular Sciences**, v. 19, n. 6, p. 1759, 13 jun. 2018.

ÚRBEZ-TORRES, J. R.; GUBLER, W. D. Susceptibility of grapevine pruning wounds to infection by Lasiodiplodia theobromae and Neofusicoccum parvum. **Plant Pathology**, v. 60, n. 2, p. 261–270, 2011.

VAN LOON, L. C.; REP, M.; PIETERSE, C. M. J. Significance of inducible defense-related proteins in infected plants. **Annual Review of Phytopathology**, v. 44, p. 135–162, 2006.

VENKITASAMY, C. et al. Grapes. In: **Integrated Processing Technologies for Food and Agricultural By-Products**. [s.l.] Elsevier, 2019. p. 133–163.

VILVERT, E. et al. Root proteomic analysis of grapevine rootstocks inoculated with Rhizophagus irregularis and fusarium oxysporum f. Sp. herbemontis. **Revista Brasileira de Ciencia do Solo**, v. 41, p. 1–14, 2017.

VOLYNKIN, V. et al. The assessment of agrobiological and disease resistance traits of grapevine hybrid populations (Vitis vinifera l. × muscadinia rotundifolia michx.) in the climatic conditions of crimea. **Plants**, v. 10, n. 6, p. 1–17, 2021.

WAALWIJK, C. et al. Synteny in toxigenic Fusarium species: The fumonisin gene cluster and the mating type region as examples. **European Journal of Plant Pathology**, v. 110, n. 5–6, p. 533–544, 2004.

WIKLUND, S. et al. Visualization of GC/TOF-MS-based metabolomics data for identification of biochemically interesting compounds using OPLS class models. **Analytical Chemistry**, v. 80, n. 1, p. 115–122, 2008.

WITTE, C. P. Urea metabolism in plants. **Plant Science**, v. 180, n. 3, p. 431–438, 2011.

WONG, J. W. H. et al. The Influence of Contrasting Microbial Lifestyles on the Pre-symbiotic Metabolite Responses of Eucalyptus grandis Roots. **Frontiers in Ecology and Evolution**, v. 7, n. FEB, 1 fev. 2019.

WONG, J. W. H. et al. Comparative metabolomics implicates threitol as a fungal signal supporting colonization of Armillaria luteobubalina on eucalypt roots. **Plant, Cell & Environment**, v. 43, n. 2, p. 374–386, 3 fev. 2020.

WUNDERLICH, L.; KLONSKY, K.; STEWART, D. **Sample costs to establish a vineyard and produce wine grapes.Sierra Nevada Foothills.**

WURZ, D. A.; FELDBERG, N. P.; BRIGHENTI, A. F. Rooting potential of grapevine rootstocks cuttings. **Revista Ceres**, v. 69, n. 1, p. 121–124, fev. 2022.

XU, X.-H. et al. Friend or foe: differential responses of rice to invasion by mutualistic or pathogenic fungi revealed by RNAseq and metabolite profiling. **Scientific Reports**, v. 5, n. 1, p. 13624, 8 nov. 2015.

YI, L. et al. Chemometric methods in data processing of mass spectrometry-based metabolomics: A review. **Analytica Chimica Acta**, v. 914, p. 17–34, 2016.

ZHANG, H. et al. Fusarium: A treasure trove of bioactive secondary metabolites. **Natural Product Reports**, v. 37, n. 12, p. 1568–1588, 2020.

ZHANG, L. et al. Transcriptomic analysis of resistant and susceptible banana corms in response to infection by Fusarium oxysporum f. sp. cubense tropical race 4. **Scientific Reports**, v. 9, n. 1, p. 8199, 3 dez. 2019.

ZHAO, H. et al. Carbohydrate metabolism and transport in apple roots under nitrogen deficiency. **Plant Physiology and Biochemistry**, v. 155, n. May, p. 455–463, 2020.

ZHOU, Y. et al. Soybean NADP-malic enzyme functions in malate and citrate metabolism and contributes to their efflux under Al stress. **Frontiers in Plant Science**, v. 8, n. January, p. 1–11, 2018.

ZIEDAN, E.-S. H.; EMBABY, E.-S. M.; FARRAG, E. S. First record of Fusarium vascular wilt on grapevine in Egypt. **Archives Of Phytopathology And Plant Protection**, v. 44, n. 17, p. 1719–1727, out. 2011.